Renewable and Sustainable Energy Reviews 114 (2019) 109300

Contents lists available at ScienceDirect

Renewable and Sustainable Energy Reviews

journal homepage: www.elsevier.com/locate/rser

Recent advances in methods and technologies for enhancing bubble detachment during electrochemical water splitting

Ghasem Barati Darband[a], Mahmood Aliofkhazraei[a,*], Sangaraju Shanmugam[b,**]

[a] Department of Materials Engineering, Tarbiat Modares University, Tehran, Iran, P.O. Box: 14115-143, Tehran, Iran
[b] Department of Energy Science & Engineering, Daegu Gyeongbuk Institute of Science & Technology (DGIST), Daegu, 42988, Republic of Korea

ARTICLE INFO

Keywords:
Renewable energy
Electrocatalyst
Bubble resistance
Hydrogen evolution reaction
Oxygen evolution reaction

ABSTRACT

Development of new electrocatalysts with high electrocatalytic activity and stability is of great importance in the production of hydrogen fuel. Numerous methods have been established to increase the activity of electrocatalysts, including increasing active surface area and improving intrinsic catalytic activity. However, the electrochemical water splitting is a gas-involving reaction in which hydrogen and oxygen bubbles are formed on cathode and anode surfaces, respectively, which lead to an increase in overpotential of electrochemical reactions. In this review, recent advances have been complied to understand the behavior of hydrogen and oxygen bubbles separation from the surface of electrodes during water splitting. Initially, various types of resistance in water splitting have been discussed, and further progress has been discussed to improve the separation of bubbles and thus improve electrocatalytic activity. These improvements include surface nanostructuring and making superaerophobic surfaces where bubbles can easily be removed from the surface, resulting in lower bubble resistance. Furthermore, the use of magnetic, supergravity and ultrasonic fields are among additional methods for fast separation of bubbles from the surface and improving catalytic activity This paper presents a review of a research pathway for creating 3D nanoarrays to improve the bubble separation behavior on the surface and improve electrocatalytic properties.

1. Introduction

Increased demand for energy, depletion of the fossil fuels and pollution of the environment due to the extensive use of carbon-emitting fossil fuels are among the main reasons for research into the development of renewable energies [1–3]. Among all the renewable fuels, hydrogen is considered one of the essential alternatives to fossil fuels [4–6]. Hydrogen can be produced using numerous methods. Some methods, such as steam reforming of fossil fuels, emit toxic gases such as CO_2 into the environment, while the produced hydrogen through this method is not pure. One of the best methods in this aspect is the electrochemical water splitting which is regarded as the cleanest way of producing hydrogen. By utilization of this approach, unlike hydrogen production from hydrocarbons, no pollution is introduced into the environment. Moreover, this method uses water as a cheap and renewable resource [7–9]. Additionally, the produced hydrogen through the electrolysis method is very pure and devoid of carbon monoxide, therefore it can be used directly for various applications such as fuel cells, and the risk of anode poisoning will be minimum [10–12]. The water electrolysis process consists of two half-reactions, which include the hydrogen evolution reaction (HER) ($2H + 2e^- = H_2$ (g)) and the oxygen evolution reaction (OER) ($2H_2O$ (l) = $O_2 + 4H^+ + 4e^-$). At first glance, it may seem that the water electrolysis reaction is a simple one. However, this reaction does not occur at its thermodynamic voltage (1.23 V) and requires a higher voltage [13,14]. Therefore, one of the most crucial research fields is the development of electrocatalytic compounds that can be used as electrocatalyst on which water can be split at the lowest potential. The most effective electrocatalysts for reducing the overpotential are the Pt-based electrocatalyst for HER, as well as the Ir and the Ru oxide based electrocatalyst for OER [15–17]. Unfortunately, the high price and the limited resources of these materials are the main constraints on their widespread usage.

Therefore, in order to improve the efficiency of the electrochemical water splitting process, an electrocatalyst with a low overpotential, high reaction rate and cost-effective is required. In general, there are various procedures for the development of high-activity electrocatalytic electrodes including the selection or construction of an electrode with a high electrocatalytic activity, which is determined by the electronic

* Corresponding author.
** Corresponding author.
E-mail addresses: khazraei@modares.ac.ir, maliofkh@gmail.com (M. Aliofkhazraei), sangarajus@dgist.ac.kr (S. Shanmugam).

https://doi.org/10.1016/j.rser.2019.109300
Received 21 February 2019; Received in revised form 23 July 2019; Accepted 24 July 2019
Available online 31 July 2019
1364-0321/

structure of active centers [18,19]. The second procedure involves the construction of high-conductivity porous electrodes, in which the electrolyte penetration and electron transfer occur more easily [20–22]. Based on these methods, different types of electrodes have been developed as electrocatalyst for water splitting. These catalysts include metallic alloys [23], phosphide [24], sulfide [19], nitride [25] and carbide [26] for HER, and oxide [27,28] and hydroxide [29] compounds for OER.

In the electrolysis reaction, many resistances need to be overcome in order to continue the water electrolysis reaction. These resistances include the resistance of external circuits, the OER overpotential, the resistance created by the formation of bubbles on the electrode, the resistance created by the electrolyte and membranes, as well as the HER overpotential and the resistance of external circuits. In the meantime, the resistance created by the formation of bubbles on the electrode can be of great importance. Briefly, when a bubble is placed on the surface, the contact between electrode and electrolyte is extremely limited, which leads to an increase in the voltage required for the water electrolysis reaction.

Despite the many advances made in the emergence of active catalysts, little research has been done to improve electrocatalytic activity by designing an effective architecture to separate bubbles from the surface. The design of effective surface engineering for the rapid separation of bubbles from the surface as designed as an active electrode to improve electrocatalytic activity can be effective and useful. In these designs, the adhesion between the surface and the bubble must be reduced, and the bubble separation rate increased from the surface [30]. Using surface engineering and imitation of nature, the adhesion between the bubble and surface can be controlled underwater. By tailoring the surface texture, surface wettability and, consequently, water and surface bubble behavior can be engineered [7,31–33]. One of these surface engineering and surface tailoring is the fabrication of superaerophobic and superhydrophilic surface. In superaerophobic surfaces, the interface between solid-liquid-gas is discontinuous, which leads to a decrease in the adhesion between the bubble and the surface, the size of the bubbles decreases when the surface is separated, thereby improving the electrocoagulation activity. On the other hand, in the superhydrophilic surface, the interface between the electrolyte and the electrode surface increases, the penetration process increases and as a result, the reactions leading to gas consumption increase [34].

Another method for improving the bubbles separation rate is using magnetic, ultrasonic, and supergravity fields during water electrolysis, along with changing the composition of the electrolyte and the design of new electrolysis water systems. The applied external fields induce the excess convection on the electrolyte, effectively reducing the harmful effects of bubble accumulation on the surface and consequently increase the catalytic activity. Due to the importance of bubble resistance and the lack of a complete and comprehensive overview of this issue, the purpose of this review article is to provide a comprehensive overview of the recent advances in bubble resistance reduction technology. Further, this review provides the importance of bubble resistance during electrochemical water splitting, researchers can design nanostructures that increase their surface area, increase the penetration rate of electroactive species, reduce bubble resistance, and ultimately, improves electrocatalytic activity.

2. Fundamentals of water electrochemistry

A typical electrolysis system is comprised of three components: the aqueous solution, cathode, and anode. When an external voltage is established between the two electrodes, HER and OER occur on the surface of the cathode and anode, respectively. Depending on the type of electrolytic solution used, the water splitting reactions can be described as follows [35]:

Overall:

$$H_2O \rightarrow H_2 + 1/2\ O_2 \quad (1)$$

In acidic solution:

$$\text{Cathode: } 2H^+ + 2e^- \rightarrow H_2 \quad (2)$$

$$\text{Anode: } H_2O \rightarrow 2H^+ + 1/2O_2 + 2e^- \quad (3)$$

In basic and neutral solution:

$$\text{Cathode: } 2H_2O + 2e^- \rightarrow H_2 + 2OH^- \quad (4)$$

$$\text{Anode: } 2OH^- \rightarrow H_2O + 1/2O_2 + 2e^- \quad (5)$$

HER and OER reactions have different steps and mechanisms that need to be carefully studied. In this section, the exact mechanism of these reactions is discussed. HER is a two-step reaction. In the acidic environments, the HER begins with the Volmer step. At this stage, the hydrogen ions adsorb the electrons, and the intermediate hydrogen atom (H*) is produced which is subsequently absorbed onto the catalyst surface, then the hydrogen is separated from the surface by the chemical combination of Tafel or electrochemical Heyrocsky steps [36]. Therefore, there are two mechanisms for HER in an acidic and alkaline environment which include the below mechanisms:

- Volmer – Tafel mechanism
- Volmer- Heyrovsky mechanism

The HER pathway in an alkaline environment is similar to that of an acid environment, with the exception that intermediate atomic hydrogen is produced in the alkaline medium by water molecules, which is described as:

$$H_2O + e^- + * \rightarrow H^* + OH^- \quad (6)$$

In an alkaline environment, unlike the acidic environment, in the Volmer process, the electrochemical reduction of H_2O should take place into absorbed OH^- and H *. In these conditions, before adsorption of H * at the catalyst surface, the H-O-H bond in the solution should be broken, which is more difficult. Therefore, for the water splitting reaction, the acidic environment is more favorable due to its H^+ content [37].

Therefore, in general, the HER routes in acidic and alkaline environments can be described as follows [38]:

In acidic solution:

$$\text{Step 1: } H_3O^+ + * + e^- \rightarrow H^* + H_2O \text{ (Volmer)} \quad (7)$$

$$\text{Step 2: } 2H^* \rightarrow H_2 \text{ (Tafel)} \quad (8)$$

$$\text{Step 2': } H_3\text{Ø}^+ + H^* + e^- \rightarrow H_2 + H_2\text{Ø (Heyrovsky)} \quad (9)$$

In basic and neutral solution:

$$\text{Step 1: } H_2O + e^- + * \rightarrow H^* + OH^- \quad (10)$$

$$\text{Step 2: } 2H^* \rightarrow H_2 \text{ (Tafel)} \quad (11)$$

$$\text{Step 2': } H_3\text{Ø}^+ + H^* + e^- \rightarrow H_2 + H_2\text{Ø (Heyrovsky)} \quad (12)$$

In general, all steps and paths depend strongly on the chemical and electronic properties of the surface of the electrode.

If the adsorption of hydrogen on the catalyst surface is very weak, then the Volmer stage will control the overall kinetics of HER, in which the Tafel slope is about 120 mV/dec. If the Volmer stage is the rate determining step, then an electrode with more cavity and edges a surface will be more effective to adsorb more hydrogen and improve the charge transfer process. However, if hydrogen adsorption is very strong on the surface of the catalyst, then the hydrogen desorption from the surface (Tafel or Heyrovsky reactions) will control the overall reaction kinetics. Thus, if the number of H* is sufficiently high on the surface, the two adjacent hydrogen atoms tend to combine resulting in the formation of hydrogen gas and subsequent release from the surface. In

this case, the Tafel reaction would control the overall kinetic reaction, where the Tafel slope is equal to 30 mV/dec. Finally, if the concentration of intermediate hydrogen atoms is low on the surface, then the Heyrovsky reaction will control the overall reaction speed, and the Tafel slope will then be 40 mV/dec [39–41].

If the Heyrovsky or Tafel reaction is the controller of the overall reaction rate, then the water splitting rate can be increased by increasing the area of the reaction, which is achieved by increasing surface roughness [14]. The Gibbs free energy of the hydrogen atom (ΔG_H) on the catalyst surface is critical to determine the inherent electrocatalytic activity. The exchange current density curve in terms of ΔG_H, known as the volcano curve, is used to determine the intrinsic electrocatalytic activity. Since the adsorption and desorption of the H atoms (H_{ads}) on the electrode surface is a competitive process, a good HER electrocatalyst must establish a suitable bond with the adsorbed hydrogen in which the electron-proton transfer process is easily carried out and, on the other hand, this bond should be weak enough to cause the bond breaking to easily release H_2 [42]. Therefore, an optimal catalyst is located in the coordinates near the vertex of the volcano curve in which ΔG_H is close to zero.

Although many studies have been done to understand the OER mechanism, the mechanism of this reaction is not fully understood at this time [35,43,44]. A proposed mechanism for OER is outlined below The OER mechanism and the pathway for the OER reaction are slightly more complicated than the HER process. This reaction is a 4 electron process which occurs on the anode surface in a water electrolysis reaction. Compared to HER, the kinetics of the OER reaction is slower. In general, the OER in an alkaline solution consists of four steps [45,46]:

$$M + OH^- \rightarrow MOH + e^- \quad (13)$$

$$MOH + OH^- \rightarrow MO + H_2O + e^- \quad (14)$$

$$MO + OH^- \rightarrow MOOH + e^- \quad (15)$$

$$MOOH + OH^- \rightarrow M + O_2 + H_2O + e^- \quad (16)$$

Firstly, OH^- ions are adsorbed on active surfaces according to reaction 13. Secondly, secondary OH^- ions are adsorbed on the surface, and then in the third step, the generated MO react with the OH^- ions resulting in the formation of MOOH. Finally, oxygen gas is produced according to reaction 16. Metal redox reactions accompany these processes. It can be said that the kinetics of OER depends on the reaction between active sites and reactive species.

3. Different resistance in the water electrolysis system

In order to begin the water splitting process, various resistances need to be overcome. It means that in addition to the thermodynamic voltage of the water electrolysis reaction (1.23 V), additional voltage is required which is termed as overpotential. In general, the purpose of designing different electrocatalysts, as well as designing different water electrolysis methods is to reduce the overpotential. Different resistances during water electrolysis reaction are shown schematically in Fig. 1. In general, these resistors can be categorized as follows:

The first resistance is electrical resistance in the electrolysis cell. These resistances exist due to the passage of electric current from external electrical circuits, which can be calculated by the Ohm's law (R = V/I), where I is current when V voltage is applied to the circuit. The resistance of the electrodes and circuits of the system is determined by the type and dimensions of the materials used in the electrolysis system, the method of preparation and conductivity of the components of the electrolysis system. This resistance can be expressed as follows.

$$R = \sum \frac{1}{AK_g} \quad (17)$$

Where, R is electrical resistance, K_g is the electrical conductivity of each component (Ω^{-1} m^{-1}), including wires, connectors, and electrodes. This resistance can be reduced by decreasing the length of the wires, increasing the cross-section, and using wires and components with high electrical conductivity [47].

The second resistance is resistance due to electrochemical reactions at the cathode and anode surface, which called activation overpotential. These resistances exist due to the overpotential needed to overcome the activation energy of hydrogen and oxygen evolution reactions on the surface of the cathode and the anode. Activation overpotential is the intrinsic property of a material used as a catalyst. This property varies from one material to another. Therefore, it is possible to reduce this resistance by choosing an effective catalyst.

The amount of electrochemical overpotential produced by the HER and OER reactions can be expressed by equations (18) and (19), respectively [48].

$$\eta_{cathode} = 2.3 \frac{RT}{\alpha F} \log \frac{i}{i_0} \quad (18)$$

$$\eta_{anode} = 2.3 \frac{RT}{(1-\alpha)F} \log \frac{i}{i_0} \quad (19)$$

Where, R is the gas constant (8.314 kJ mol^{-1} k^{-1}), i_0 is the exchange current density, F is Faraday constant (96485 C mol^{-1}), α is the symmetry factor and T is the temperature. The amount of overpotential created on the cathode surface directly relates to the formation of the hydrogen on the near of cathode surface. The formation of hydrogen on the cathode surface depends on the formation of the bond between hydrogen and the surface of the electrode, which is intrinsic property.

Another important resistance is resistance due to bubbles phenomena. When hydrogen and oxygen bubbles are formed on the surface of the cathode and the anode, the bubbles must be removed from the surface. However, if these bubbles cannot be easily removed from the surface, the area between the surface and the electrolyte is decreased. This leads to the blocking of the surface of the site, consequently creating an additional overpotential on the surface. This resistance is known as the bubble resistance. Bubble phenomena and bubble resistance will be discussed further in the following sections.

Finally, another resistance is the mass transfer resistance in the water electrolysis system. This resistance exists. This resistance exists due to the transfer of ions in the electrolyte, as well as to the membranes created for the separation of hydrogen and oxygen. The ionic transfer resistance created by the transfer of ions in the electrolyte depends on the electrolyte concentration, the distance between the anode and the cathode, and the distance between the diaphragm and the electrodes. Although mass transfer leads to an increase in the rate of electrochemical reactions, it does not always mean much hydrogen production. A large amount of hydrogen bubbles produced by the high reaction rate can prevent contact between the electrode and the electrolyte. To reduce this resistance, the electrolyte conductivity can be increased, or the appropriate additives can be added in the electrolyte [14].

3.1. Bubbles phenomena during water electrolysis

As was previously stated, during the water electrolysis, hydrogen and oxygen gases are formed on the surface of the electrodes, and they can only be separated from the surface upon reaching sufficient size. The coverage of the electrode surface by the formed bubbles can increase the total resistance of the system, resulting in a reduction of the interface between the electrode and the electrolyte. Therefore, the accumulation of bubbles increases the amount of the overpotential required for electrolysis of water. As a result, understanding the bubble phenomena on the surface of the electrode and its effective rules can help in the fabrication of suitable electrocatalysts, as well as the design of the water electrolysis system. It has been shown that by increasing the surface covered by the bubble, the amount of overpotential required for water electrolysis is greatly increased. Moreover, the bubble layer created on the surface greatly reduces the gas evolution [49]. Since the surface covered by bubbles reduces the active area, the potential for

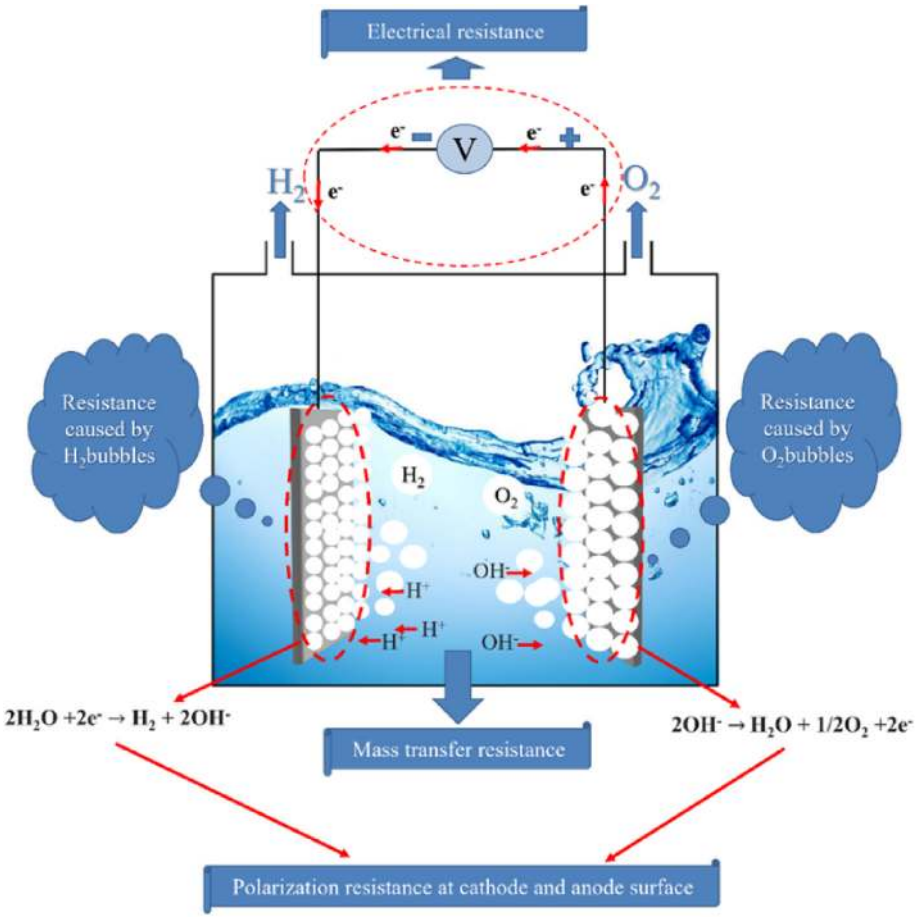

Fig. 1. Schematic presentation of different resistance during water electrolysis.

HER can be expressed as follows [50]:

$$\eta_\theta = \eta + b \log (1/1\text{-}\theta) \quad (20)$$

In which η_θ is the overpotential with the effect of the bubbles taken into account, η is the overpotential without effect the bubbles, and θ is the ratio of surface coverage by the bubbles, varying between 0 and 1. Given eq (20), it is discovered that by increasing the surface covered by the bubbles, the amount of the final overpotential is also increased.

Understanding the dynamics of bubble behavior on the surface is vital for determining the conditions of separating the bubble from the surface. The bubble contact angle on the surface inside the water is defined as the Yang equation [51,52]:

$$\cos\theta_b = \frac{\gamma_{sv} - \gamma_{sl}}{\gamma_{lv}} \quad (21)$$

where γ_{sv}, γ_{sl} and γ_{lv} are surface tension of solid/vapor, solid/liquid and liquid/vapor, respectively. Once the bubble can be removed from the surface, the solid/liquid interface is replaced with the solid/vapor interface. The Gibbs free energy changes are defined as the following in order to replace a unit of solid/liquid with solid/vapor interface [53].

$$\Delta G = \gamma_{lv}(\cos\theta - 1) \quad (22)$$

Therefore, it can be stated that the separation of the bubble from the surface depends on the displacement of the electrolyte in the solid/liquid interface, which is known as wettability [54]. In addition to creating resistance due to the formation of bubbles on the surface, the formation of bubbles on the surface leads to a decrease in concentration polarization [55]. During the electrochemical process at the electrode surface, the electrolyte is saturated from the product of the electrochemical reaction near the electrode. Such an increase in the concentration of products near the surface of the electrode leads to a polarization concentration (η_C) [55].

$$\eta_C = \frac{RT}{nF} \ln \frac{C_g}{C_g^{sat}} \quad (23)$$

where, C_g is the concentration of dissolved-gas at the interface and C_g^{sat} is the saturation concentration. Studies have shown that the formation of bubbles on the surface leads to an increase in mass transfer and thus decreases concentration polarization [56,57]. Thus, we examine the effect of the resulting bubble on the surface of the formation of the resistance. However, further studies to determine the effect of the bubble on the decrease of concentration polarization and, consequently, the improvement of the rate of gas involving electrochemical reaction is needed and should be carefully examined.

3.2. Bubble separation behavior from the surface

Before discussing the development of bubble separation strategies from the electrode surface, a careful study of the bubble behavior separation from the electrode surface during the water electrolysis reaction is required. In general, a bubble can be removed from the surface and penetrate the electrolyte when its diameter reaches a critical value [58,59]. Schematic represents the separation of hydrogen and oxygen bubbles is shown in Fig. 2. The motion direction of the bubbles is along the x and z-axes. The motion in the x-direction is due to the difference in the concentration of gas bubbles in the electrolyte, whereas movement in the z-direction is due to the density difference between the gas bubble and the electrolyte. Therefore, the resultant force in the x and z-direction determines the direction of motion of the gas bubbles. If the bubble separation rate is low on the surface of the electrode, a layer of

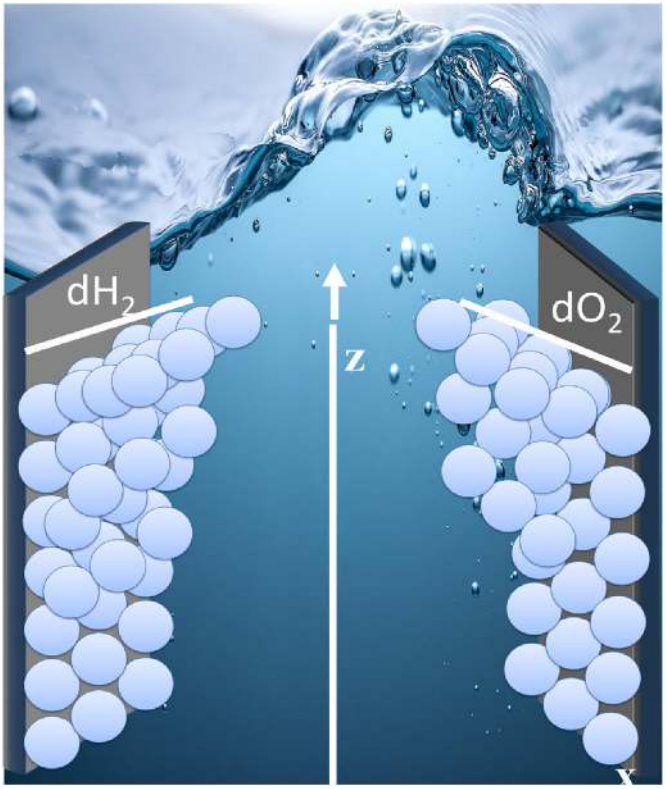

Fig. 2. Schematic representation of the separation of hydrogen and oxygen bubbles from the surface during water splitting.

bubbles is formed on the surface, and its thickness will be a function of its height. As the schematic figure indicates, with increasing height, the thickness of this layer is also increased. The low separation rate of the bubbles will increase the effect of the bubble, which will increase the IR drop, consequently increasing the overpotential. This is one of the essential sources of an energy boost in the water electrolysis reaction.

4. Strategies for reducing the bubble effect during water electrolysis

In general, the strategies for reducing the resistance created by the bubble phenomenon can be schematically in Fig. 3.

4.1. Superaerophobic surface

4.1.1. Fundamentals of superaerophobic surface

In general, the air bubble contact angle on an ideal surface immersed in water depends on the contact angle of a sticking droplet (θ_w) on a similar surface in the air. By knowing the contact angle of the water, the contact angle of the bubble on a flat surface immersed in the water can be predicted. When a surface is immersed in an aqueous medium, water molecules near the surface of the substrate and air bubbles trying to stick to the substrate must compete with a film on the surface. Thus, similar to a drop of water on the solid surface in the air, the intermolecular forces between the various phases (solid/water and solid/air) will determine the behavior of the bubbles in water. The bubble contact angle can be obtained using the Yang equation, which was mentioned in equation (24). The water contact angle (θ_w) and the bubble angle (θ_b) are related to each other through the following equation [60]:

$$\theta_b = 180 - \theta_w \tag{24}$$

According to the equation above, it can be argued that a superhydrophilic surface is a super aerobic surface under water and vice versa. The relationship between the wettability of solid substrates in the air and aqueous media is shown in Fig. 4.

Another physical parameter that can be used to express the wettability of the air bubble is the hysteresis contact angle (CAHb), which is, in fact, the difference between the maximum cos and the minimum static contact angle, when the substrate is tilted to any given angle. Surfaces with the bubble contact angle greater than 150° have a low hysteresis and are known as superaerophobic surface [52,61–63]. On the other hand, surfaces with smaller bubble contact angle possess higher hysteresis angles, which are known as superaerophilic surfaces.

If the surface energy of a structure with a micro-nanoscale roughness is reduced, then a superhydrophobic surface is created at which water is repelled by surface and the contact angle of the water is greater than 150° while the hysteresis contact angle is less than 5° [64–66]. At these surfaces, air is trapped inside the rough texture. Therefore, it can be stated that if the gas bubble is in contact with these superhydrophobic surfaces, trapped air on the surface of the aforementioned hydrophobic structure can easily be mixed with the gas bubbles, leading to the spread of gas bubbles on the surface and creation of a superaerophilic surface that has a bubble contact angle smaller than 5°. On hydrophilic surfaces, the capillary force causes water to penetrate into the surface roughness, and as a result, when a gas bubble comes into contact with such a surface, it can remain on the surface and almost resemble a sphere on the surface to move freely [67,68].

Consequently, a superaerophobic surface is created. Another important parameter in the phenomenon of superaerophobic surfaces is the adhesion force on the surface of the bubbles, which is calculated in most of the issues related to the phenomenon of superaerophobicity [51]. The bubble adhesion on the surface depends on the volume of the bubble and CAHb. The relationship between the various parameters and $F_{adhesion}$ is given below [51]:

$$F_{adhesion} = kd_{\gamma lv}(\cos\theta_{\min} - \cos\theta_{\max}) \tag{25}$$

In this equation, k is equal to the retentive force factor and γ_{lv} is equal to the surface tension of the liquid. The equation states that the decrease in the bubble wettability will lower the surface of the bubble contact on the surface (d), subsequently reducing the adhesive force. This issue will be extremely influential on the electrocatalytic stability, which will be addressed in the later sections.

4.1.2. Using superaerophobic surfaces for bubble separation

In general, the process of separating gas bubbles during the water electrolysis reaction can be divided into two stages. First, small bubbles are formed on the active surfaces of the substrate in a preferential manner where surface properties generally determine the separation rate. Overall, hydrophilic surfaces are useful for rapid separation of bubbles. In addition, surface modifications are one of the most effective procedures for separating bubbles by reducing the contact interface of the bubbles and the surface of the electrode. These modifications include the use of nanoneedle, nanosheet and nanocone structures [69–72]. As soon as the small bubbles are separated from the surface, they form larger bubbles with each other throughout the second stage and become trapped in the cavity structure during the transfer from the electrode to the electrolyte. The separation rate of these large bubbles from within the cavity structure is very impactful in electrocatalytic performance [73]. The longer the bubbles remain in the cavity, the more electrocatalytic properties are affected. One of the topics that has lately attracted a lot of attention in increasing the separation rate of bubbles from the surface, has been the creation of superaerophobic surfaces. Recently, a lot of efforts have been made to obtain underwater superaerophobic surfaces through the fabrication of hierarchical micro-nanoscale surfaces [74,75]. The fabrication of superaerophobic surfaces will cause the bubbles to separate from the surface as soon as they are formed, and thereby the water electrolysis overpotential will be decreased. In this section, studies have been conducted to create superaerophobic surfaces to reduce bubble resistance.

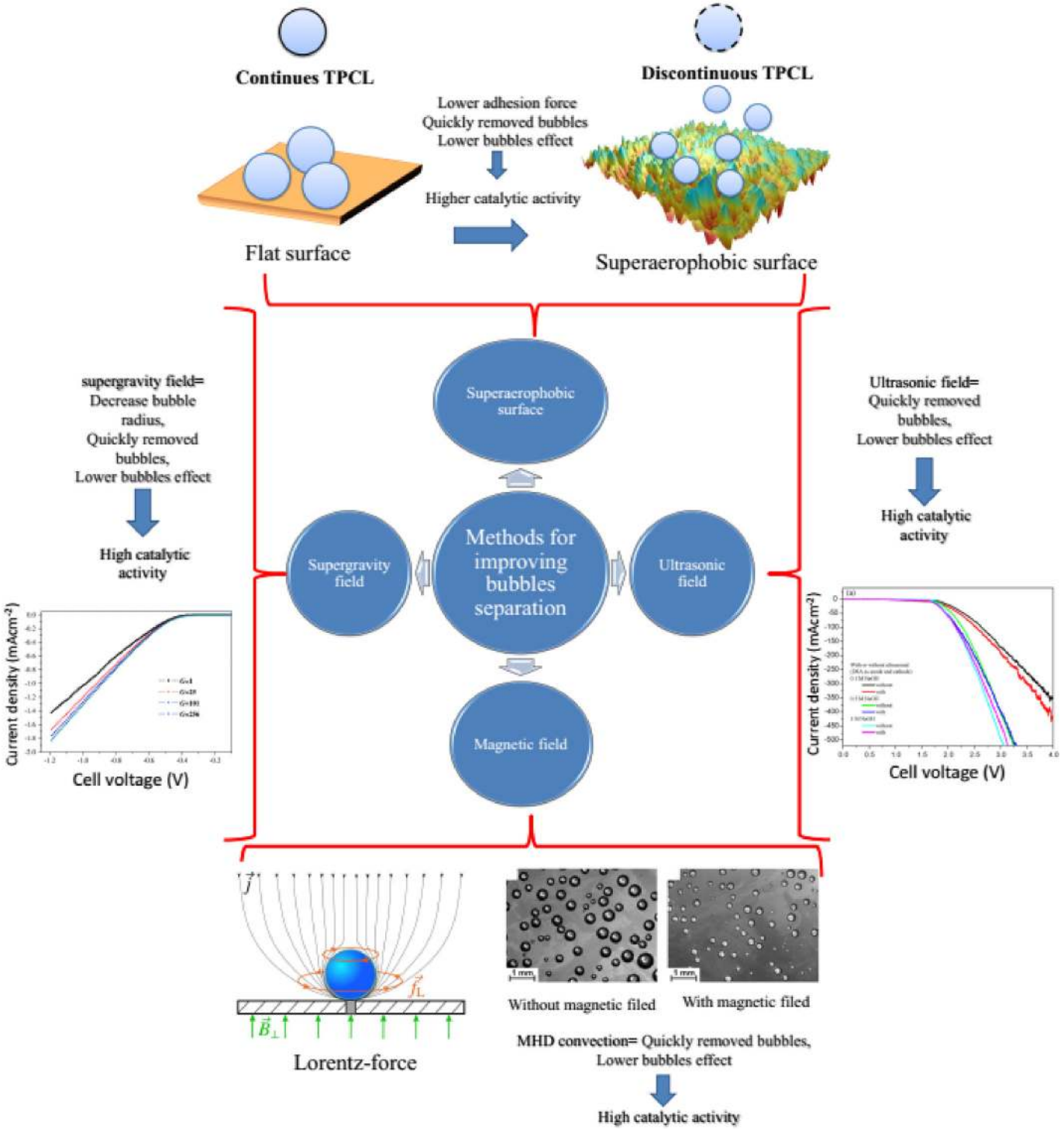

Fig. 3. Schematic representation of different methods for improving the bubble separation from the electrode surface during water splitting.

Superaerophobic surfaces have been used in order to reduce the bubble resistance in the water electrolysis reaction [69,76–81]. Furthermore, superaerophobic surfaces have been utilized to reduce bubble resistance for other electrocatalytic reactions, such as Direct Hydrazine Fuel Cells [34,82,83] and Chlorine evolution reaction [84]. Different arrays have been employed to create superaerophobic surfaces for the elimination of the negative effects of the bubbles. These arrays include vertical nanosheets [85] and pine-shaped monolayers [78] as well as nanoflower shaped structures [82]. We will discuss the effect of different nanostructure morphology of superaerophobic surfaces for easy bubbles detachment and consequently improving catalytic activity is summarized.

4.1.2.1. Nanosheets structure. Nanosheets architecture are one of the nanostructures that can be used to create superaerophobic surfaces and thus increase the bubble release rate during electrochemical water splitting. Nanosheets can be fabricated using various methods such as electrodeposition, hydrothermal, and chemical methods. Nanosheets leads to an increase in the active surface area and also leads to the division of the interface between the bubble and the surface into

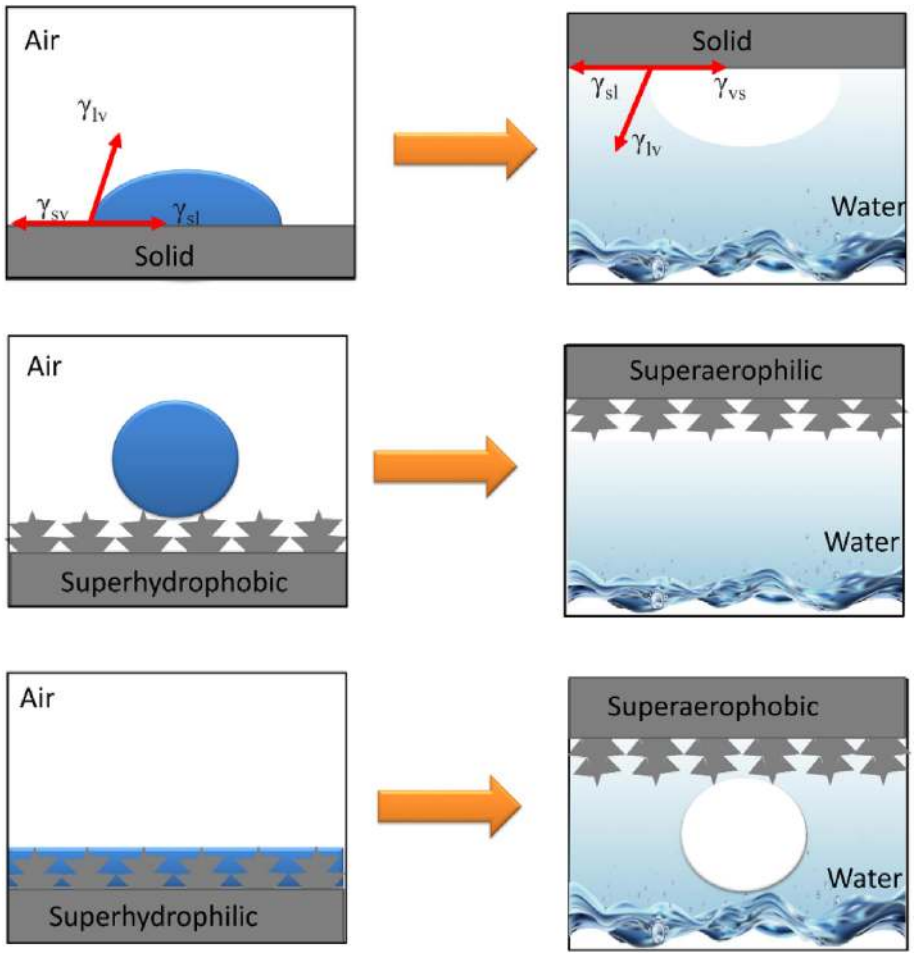

Fig. 4. Schematic showing the relationship between the wettability of solid substrates in air and aqueous media.

discontinuous parts, which causes the size of the bubbles to decrease during the separation from the surface of the electrode, which lead to decrease the bubbles and ultimately the electrocatalytic activity improves. As stated, two important factors affecting the electrocatalytic activity are the high surface area and increasing the intrinsic activity. Increasing the intrinsic electrocatalytic activity can be achieved by using materials that are inherently high in electrocatalytic activity or by doping active elements. So if we can synthesize materials that are inherently high in electrocatalytic activity in nanosheets structure, then we can observe high electrocatalytic activity. We will describe some important advances in these research areas.

One of the materials inherently have good in electrocatalytic activity is MoS_2, which has been synthesized in various forms, such as nanosheets and nanoparticles [86–88]. Also, the superaerophobicity of these materials in the nanosheet condition was studied to improve electrocatalytic activity. Lu et al. [89] developed MoS_2 nanostructures with underwater superaerophobic properties and explored as the HER electrocatalyst. Fabrication schematics of this nanostructure is shown in Fig. 5a. The smooth and non-rough surface of MoS_2 was selected for the sake of comparison. The adhesion force of structures was measured and shown Fig. 5b and c. The adhesion force of the smooth surface and without roughness was about 124.8 μN, which is quite substantial. This great amount of force applies sizeable amounts of deformation to the surface when the bubble is separated from the surface. This structure also causes the gas bubble to remain on the surface, causing a bubble locking effect on the surface. In the MoS_2 nanostructure, where the nanosheets are grown vertically on the surface, the three-phase contact line (TPCL) is not continuous, it is divided into numerous parts, and the measured adhesion force is about 10.8 μN. This facilitates the detachment of the bubbles from the surface and does not create a deformation on the surface upon removal. The MoS_2 nanostructure has a hydrophilic nature (water contact angle of 52.3° (Fig. 5d)), which makes it easy to water the surface so that it can create a water cushion using capillarity. The water cushion, as a buffer layer, reduces adhesion between bubbles and nanostructures. The bubble contact angle for the obtained nanostructure was 153.6° (Fig. 5e). The nanostructure used as the electrocatalyst for HER, the LSV curve of the MoS_2 nanostructure along with the smooth MoS_2 structure as well as platinum is represented in Fig. 5f. For the MoS_2 nanostructure, the onset potential of HER was 150 mV, while the amount of exchange current density equal to$3.87\ 10^{-7}$ and the Tafel slope was very low at 51 mV/dec. Furthermore, similar values were obtained for the smooth structure of MoS_2, which indicates similar active sites in both structures. The main difference in the rate of current is increased along with an increase in the potential. It is observed that by boosting the potential for the nanostructured sample, the current is increased rapidly. Therefore, the improvement of electrocatalytic activity can be attributed to the decrease of bubble resistance. The decrease of bubble-induced resistance has been confirmed by measuring bubble size. The resulting nanostructure was more stable than the smooth structure, which is due to the decrease of the applied force from the evolved bubbles (Fig. 5g).

Ni-Mo alloys have attracted much attention to the use of HER electrocatalyst due to the similar electronic surface state of the platinum. Therefore, if this alloy can be made in the form of a nanostructure, then, in addition to the excellent thermodynamics for HER, it would also have a great HER kinetics. Ni-Mo nanosheets were developed was developed using the topotactic process with superaerophobic properties which were later employed as an electrocatalyst for HER., At

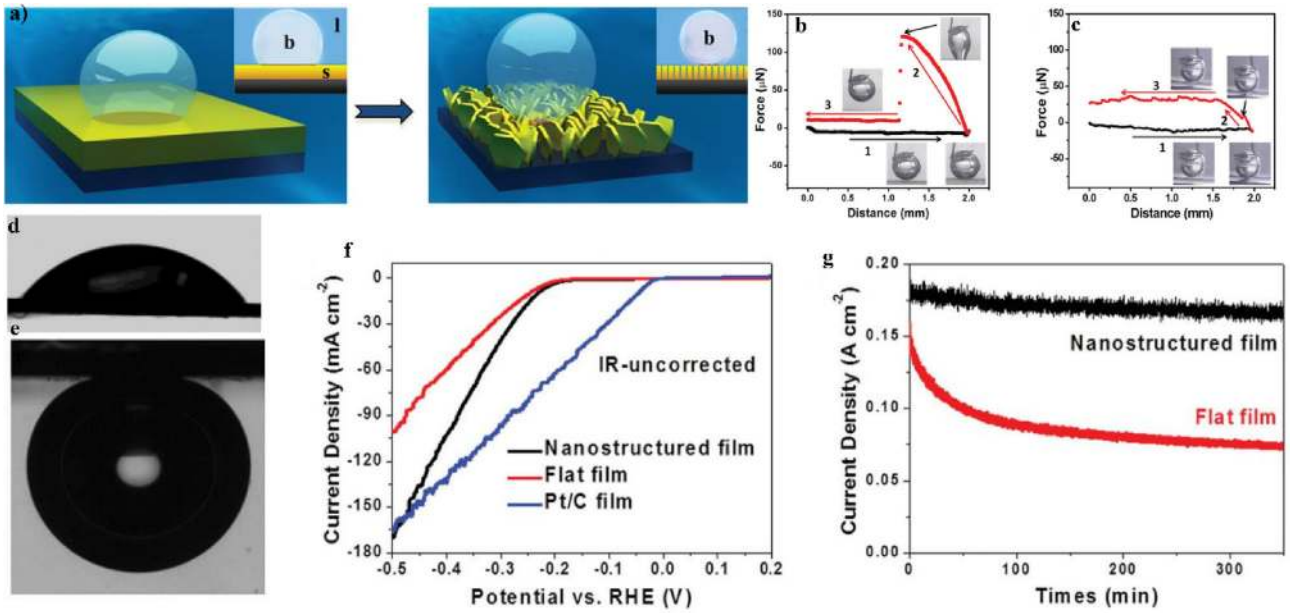

Fig. 5. a) schematic of MoS_2 nanostructure fabrication, b) adhesion force of smooth surface, c) adhesion force of nanostructure surface, d) water contact angle of nanostructure surface, e) bubble contact angle of nanostructure surface, f) LSV curves of different samples and g) chronopotentiometry curves of nanostructure and flat film [89].

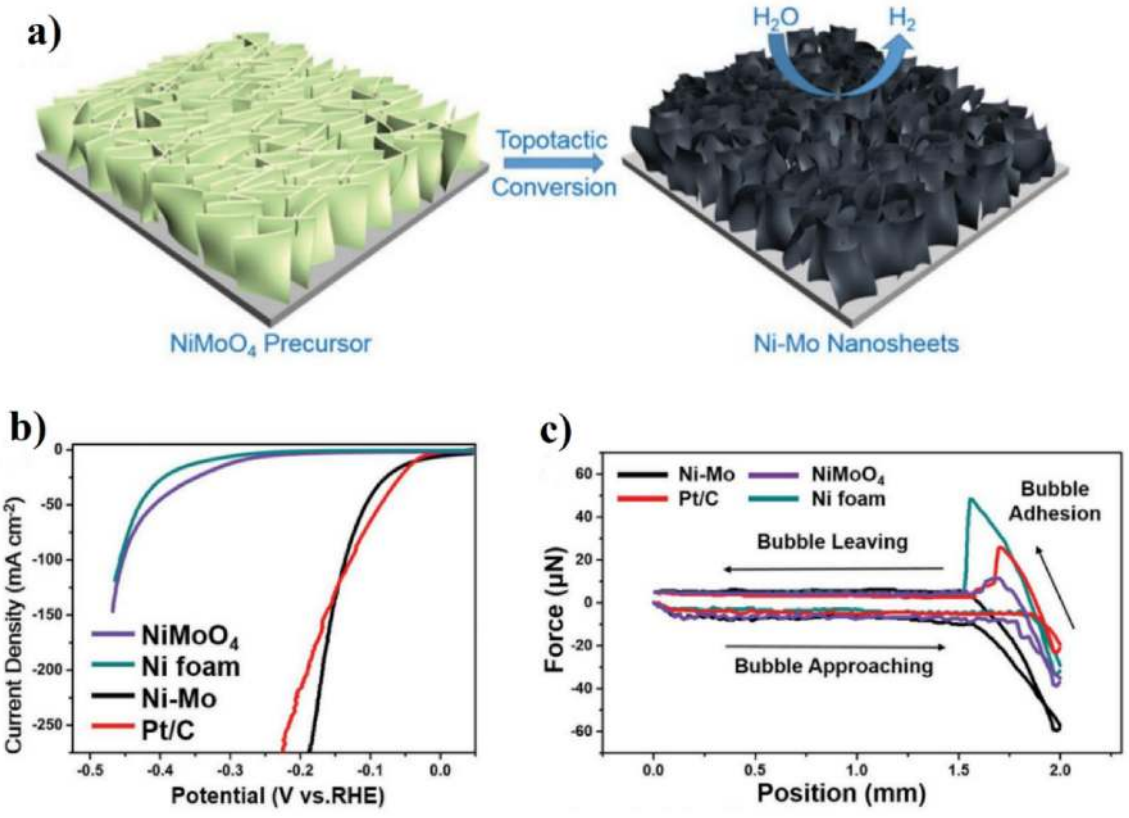

Fig. 6. a) Schematic shows the fabrication of Ni-Mo nanosheets, b) LSV curves of nanostructure surface and other electrodes and c) adhesion force measurement of different electrodes [90].

first, $NiMoO_4$ nanosheets were created. Afterwards, the Ni-Mo nanosheets were fabricated using the topotactic conversion process, as shown in Fig. 6a. The HER electrocatalytic properties of the formed electrode were studied in a 1.0 M KOH solution. The LSV curve of Ni-Mo nanostructure surface and other electrodes is presented in Fig. 6b. It is noted that to generate a current density of 10 mA cm^{-2} on the surface of this electrode, an overpotential of 35 mV is required, whereas an overpotential of 136 mV is required to generate a current density of 100 mA cm^{-2}. With the increase of the overpotential, the current density of the Ni-Mo nanostructure is enhanced sharply, and in this case, the performance of the Ni-Mo nanosheets is better than that of Pt. Therefore, it can be concluded that the mass transfer of Ni-Mo

Table 1
Comparison of electrocatalytic activity of different nanosheets structure.

Catalyst	Type of nanostructure	HER activity	OER activity	Overall water splitting	b (mV/dec)	Ref
MoS_2	Nanosheets	η_{10} = 230 mV				[89]
Ni-Mo Alloy	Nanosheets	η_{10} = 35 mV			HER = 45	[77]
Copper Phosphide	Micro sheets	η_{10} = 130 mV	η_{10} = 290 mV		HER = 83 OER = 84	[76]
Fe-Doped Ni_2P	Nanosheets	η_{50} = 214 mV	η_{50} = 230 mV	i_{10} = 1.49 V	OER = 55.9	[91]
P-$Ni(OH)_2/NiMoO_4$	Nanosheets	η_{100} = 223 mV	η_{10} = 270 mV	i_{10} = 1.55 V	HER = 130	[93]
Ni-Co-P	Nanosheets	η_{10} = 57 mV			HER = 69	[94]
Co–B–P	Nanosheets	η_{10} = 42 mV			HER = 42.1	[95]
NiCoP	Nanosheets	η_{50} = 133 mV	η_{50} = 308 mV	i_{50} = 1.77 V	HER = 68.6	[92]

nanosheets is carried out rapidly and its performance in the high current density is much better than that of Pt. On the surface of the Ni-Mo nanosheets, the three-phase contact lines between the gas bubbles and surface are discontinuous, which can significantly weaken the adhesion between the bubbles and surface of the electrode. As a result, separation of the bubbles from the electrode surface is accelerated. The bubble adhesion force test was performed in order to prove the superaerophobic state of Ni-Mo nanosheets, and the results are shown in Fig. 6c. It is observed that Ni-Mo nanosheets have a negligible bubble adhesion force in comparison with other electrodes (approximately equal to 2 μN), while this force is about 15 orders of magnitude smaller than the platinum electrode. Consequently, the catalytic activity for HER is improved on the Ni-Mo surface through the constriction of the superaerophobic surface [90].

As stated, one way to improve the inherent electrocatalyst activity is to doping the elements in the structure. Doping of the elements leads to a change in surface electronic properties and thus improves electrocatalytic activity. On the other hand, the use of an electrode that can simultaneously act as HER and OER catalyst in an electrolyte can make much progress in the production of hydrogen. One of the most important compounds that can act as bi-functional electrocatalyst is metal phosphide. If it is possible to synthesize metal phosphides as nanostructures and, on the other hand, improve their intrinsic electrocatalytic activity, then it would be possible to expect excellent thermodynamics and HER kinetics. One of the elements that can be doped into a phosphate structure is to improve the inherent catalytic activity, Fe-Ni_2P nanosheets have been created using a hydrothermal method, and iron is also doped to improve the intrinsic electrocatalytic activity [91] this electrode used as overall water splitting electrocatalyst. This electrode showed optimal electrocatalytic properties in terms of its excellent electrocatalytic properties, requiring only 230 mV overpotential to generate a current density of 50 $mAcm^{-2}$ in the OER, and only 214 mV to create a current density of 50 $mAcm^{-2}$ for HER. Additionally, only about 1.49 V is required to create a current density of 10 $mAcm^{-2}$ for the overall water splitting reaction. Such good electrocatalytic activity was attributed to superaerophobic properties.

Another element that can be doped in the Ni-P structure, which leads to the improvement of the electrocatalytic intrinsic activity, is Co-NiCoP triple nanosheets were created using the hydrothermal method, and their electrocatalytic properties were investigated for OER and HER [92]. The results indicated that for the generation of 50 $mAcm^{-2}$ current density on the surface of this electrode under optimum conditions, HER and OER require an overpotential of 133 and 308 mV respectively, which is attributed by excellent intrinsic electrocatalytic properties, rapid electron transfer, and a unique structure with superaerophobicity.

Transition Metal Hydroxides and oxides of metals are among the best candidates for the fabrication of stable and excellent electrocatalysts of overall water splitting. However, the bubble resistance caused due to bubbles formation on the surface of these electrodes is still one of the major problems Nanosheets composed of nickel hydroxide and oxide-molybdenum doped with phosphorus (P-doped Ni $(OH)_2/NiMoO_4$) was developed on nickel foam, which exhibited superaerophobic properties [93]. Electrocatalytic studies indicated that the composite possessed excellent electrocatalytic properties, which requires 60 mV overpotential to generate a current density of 10 $mAcm^{-2}$ for HER, whereas when this electrode used for overall water splitting, the voltage required to generate a current density of 10 $mAcm^{-2}$ was equal to 1.55 V. One of the most important reasons for the good electrocatalytic properties of this electrode is its superaerophobic property. It was mentioned that nickel foam has low contact angle (133°) and a high adhesion force of 23 μN. Therefore, it can be expected that the bubbles formed on the surface of the nickel foam, such as the pin, are located on the surface of the nickel foam, and do not detach from the surface and can increase the hydrogen overpotential. It is also observed that the surface of the electrode (P-doped $Ni(OH)_2/NiMoO_4$) has a superaerophobic state with a contact angle of 153° and adhesion force of 0.5 μN, which is helpful for rapid separation of the bubbles from the surface, resulting in significant reductions in the overpotential. In summary and a general comparison of electrocatalytic activity of different nanosheets, the structure is summarized in Table 1.

The creation of nanosheets led to a decrease in bubble-induced resistance and, as a result, improved electrocatalytic activity was observed. On the other hand, the creation of nanosheets did not change the onset potential. Therefore, it can be concluded that the creation of nanosheets does not change the thermodynamics of HER and does not intrinsically improve electrocatalytic activity. The important effect of nanosheets is to improve the kinetics of HER, which leads to an increase in kinetics due to lower bubble size and increased bubble separation rate. Also, one of the most important factors to improve catalytic stability is morphological stability. Generally, when the bubbles are removed from the surface, they apply a force to the surface, which is directly related to the size of the bubble when it separates from the surface. No matter how much the bubble is reduced, then the amount of force applied by the bubble to the surface decreases. Due to the decrease in bubble size with nanosheet, the amount of force applied by the bubble to the surface decreases, resulting in reduced damage, which results in morphological stability and ultimately improves electrocatalytic stability.

4.1.2.2. Nanocones structure. Another nanostructure that can effectively increase the active surface area is nanocones. Metallic nanocones can be created by electrodeposition method. On the other hand, because the nanocones structures have sharp edges, they can create a superaerophobic surface. Also, these nanocones can cause discontinuous condition the interface between the bubble and the electrode surface and, as a result, reduce the diameter of the bubbles during separation from the surface. This reduces the resistance caused by the bubble and improves electrocoagulation activity. The usage of nanocones structure to increase the active surface area, as well as to improve the behavior of bubble separation, has been the topic of our studies [7,20,96]. In one study [96], nanocomposite Ni-CNT nanocones were developed using the electrodeposition method, and their

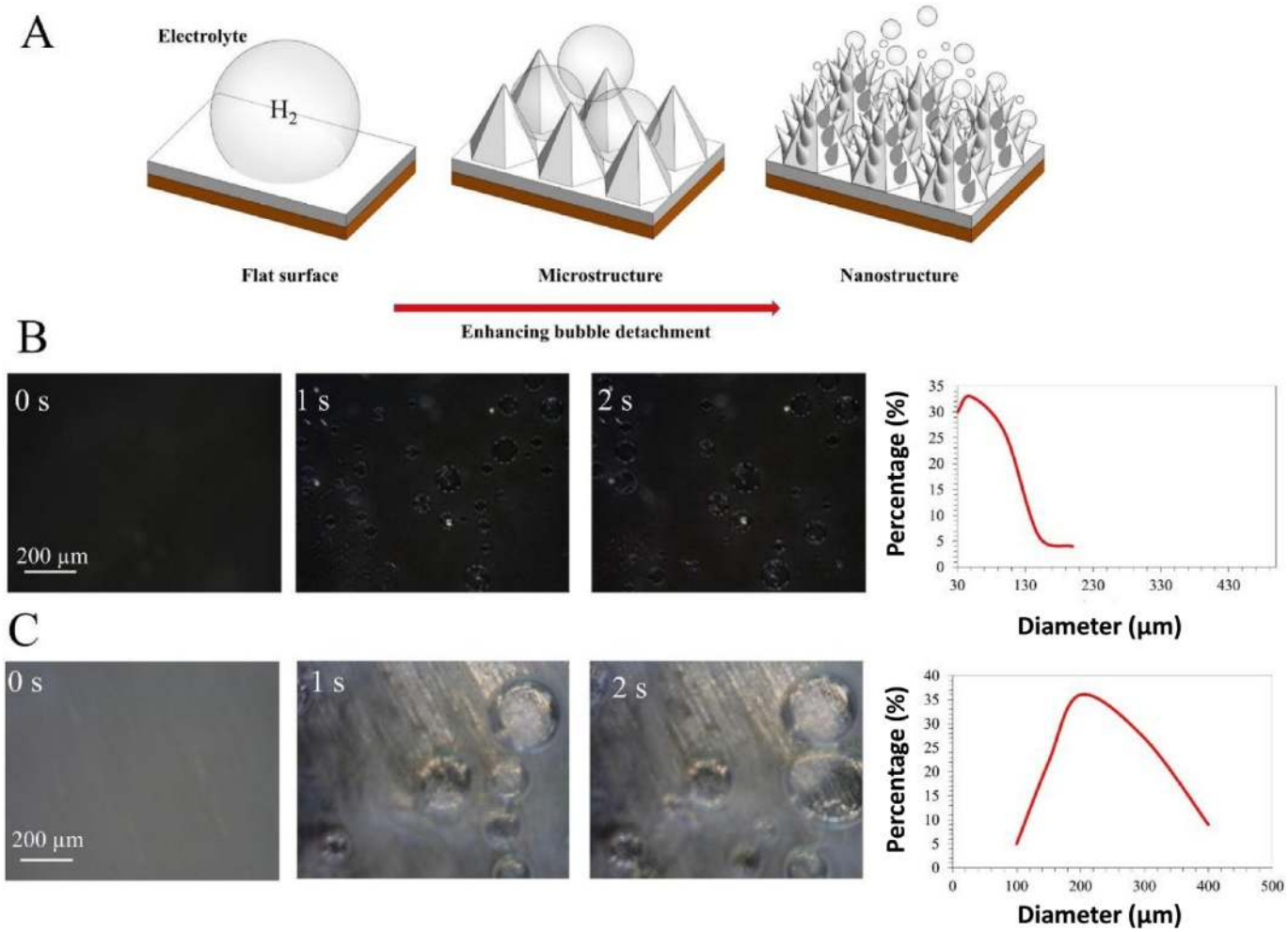

Fig. 7. A) Schematic of the bubbles detachment behavior of different structures, B) bubbles images at different intervals during the hydrogen evolution on nanocones structure, and C) bubbles images at different intervals during the hydrogen evolution on the flat surface [96].

electrocatalytic activity was investigated for HER. The results indicated that the formation of Ni-CNT nanocones resulted in a substantial enhancement in the electrocatalytic activity, in which the current density of 10 mA cm-2 required 82 mV overpotential. One of the important reasons for improving the electrocatalytic activity of this electrode was the easy separation of bubbles from the electrode surface. The schematic behavior of the separation of bubbles on smooth surfaces, microstructures, and nanostructures is shown in Fig. 7 A. Moreover, the size of the bubbles at different intervals on the smooth and nano-structured surfaces is illustrated in Fig. 7B and C. The size of the bubbles on the nanocones surface is much smaller than the smooth surface, which leads to a decrease in bubble resistance and an improvement in electrocatalytic activity. Also, improving the electrocatalytic activity of the nickel-cobalt alloy nanocones compared to other nickel base electrodes was associated with the easier separation of hydrogen bubbles from the surface of the nanocones and the increased active surface area [20]. Also, in order to improve the inherent electrocatalytic activity, Ni-Fe-Co alloy nanocones were formed, and their electrocatalytic activity was investigated for HER and OER. Due to the high surface active area, high intrinsic electrocatalytic activity and the rapid separation of the bubbles from the surface, it exhibited the excellent electrocatalytic activity of 10 $mAcm^{-2}$ current density for HER and OER, 91 mV and 316 mV overpotentials were needed. It was also needed 1.6 V to generate a current density of 10 $mAcm^{-2}$ in total water splitting.

As stated, metal phosphide-based materials are among the best bifunctional electrocatalyst for HER and OER reactions. Because it is not possible to form metallic phosphides using electrodeposition, it is possible first to create nickel metal nanocones and then a thin layer of metallic phosphide on the surface of the nanocones and obtain metallic nanocones. In a study, first, nickel nanocones were formed, and then by CV electrochemical deposition method, a thin layer Ni-Co-P was formed on the Ni nanocones.

The schematic presentation of this nanostructure is shown in Fig. 8. Due to the high active surface area resulting from the deposition on the surface of the nanocones, the high inherent electrochemical activity caused by metallic phosphide, as well as the very low resistance caused by the presence of bubbles on the surface, the intrinsic electrocatalytic activity of the fabricated electrodes was excellent in which η_{10} = 51 mV for HER and η_{10} = 221 mV for OER. Also, this electrode was used as a bifunctional catalyst in water splitting system in which require only 1.53 V to generate the current density of 10 $mAcm^{-2}$ [53]. The performance of different nanocones structure that has used for increasing the catalytic activity for HER and OER is summarized in Table 2.

4.1.2.3. Other nanostructures. In addition to the expressed nanostructures, in order to improve the electrocatalytic activity, other nanostructures have also been used to quickly disassemble bubbles from the surface, including nanotube, nanowire, and nanoflakes. In this section, we describe the effect of these nanostructures on the electrocatalytic activity for HER and OER. In order to reduce the bubble resistance and improve the separation of hydrogen bubbles from

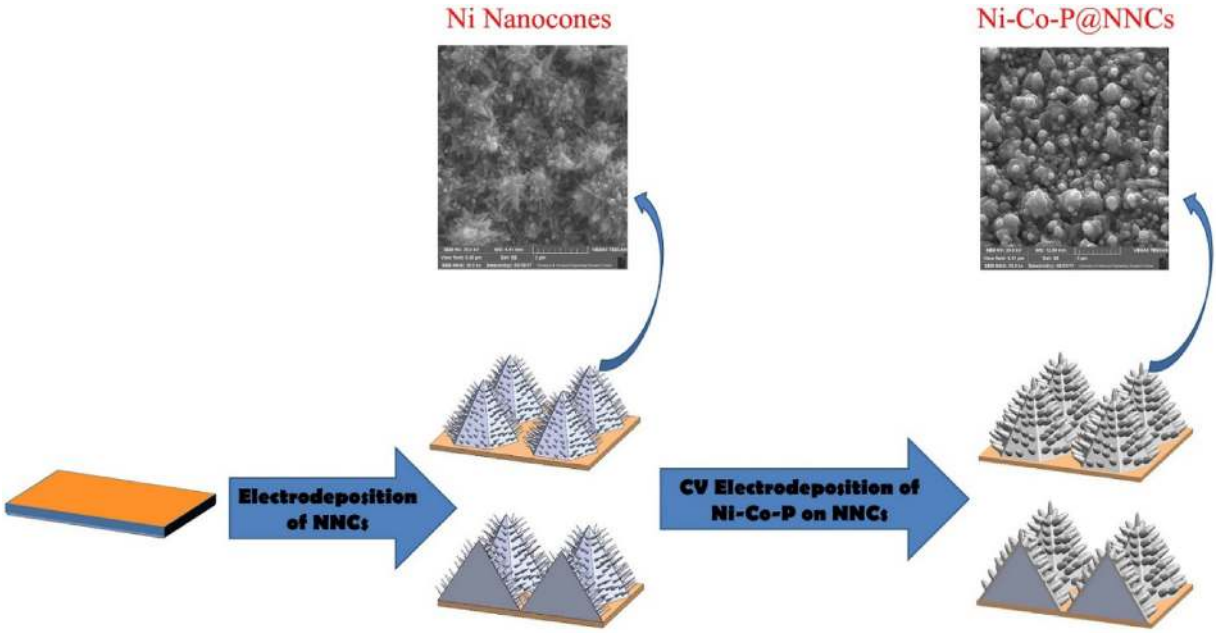

Fig. 8. Schematic showing the formation of Ni-Co-P@NNCs electrode [53].

the surface of the electrode, Li et al. [78] developed a pine-shaped platinum nanostructure using the electrodeposition process and used the electrode as HER electrocatalyst in alkaline solution. The lower adhesion force on the surface (11.5 μN) along with the higher the contact angle of bubbles in the aqueous medium (161°) and the smaller the size of bubbles upon detachment from the pine-shaped nanostructure, has led to an improvement in the electrocatalytic properties of this electrode compared to other electrodes.

As was stated, the bubble separation behavior from the electrode surface has a significant effect on electrocatalytic properties and was therefore thoroughly investigated. The shape of the bubbles, as well as their size distribution, is shown on the surface of the three structures are shown in Fig. 9. It is observed that the bubbles are quickly separated from the surface of the platinum nanostructure before their size reaches 150 μm. While the size of the bubbles is higher on the surface and linger mostly on the surface, resulting in the blockage of the surface and weakening of the electrocatalytic properties. Moreover, in this study, the better electrocatalytic stability of platinum nanostructures was associated with less scratch/drag force in comparison to other structures.

In order to effectively use a substrate for electrolysis of water, the substrate needs to possess a high surface area, excellent conductivity and a high chemical and mechanical stability [99–102]. In general, three-dimensional porous structures have been employed in various research sources as substrates. These substrates increase the active surface area, while also reducing the ion penetration pathway, effectively increasing the transfer of ions to the interior of the substrate and thus improving ECSA [103]. Even though the fact that these substrates cause increased surface activity, there is a problem of separating the bubble from the surface of the electrode due to the structure of the complex pores. Wang et al., [104] developed a new strategy to improve the behavior of bubble separation from the electrode surface during water electrolysis. They used nonwoven stainless steel fabrics as a conductive substrate for the deposition of LDH Ni-Fe nanosheets. In this research, stainless steel fibers were bonded to each other by a heat treatment called nonwoven. Each of the stainless steel fibers was decorated with Fe-Ni nanoparticles LDH, which act as surface active agents for water electrolysis. The results of this study indicated that the Fe-Ni LDH@NWSSF electrode causes the bubble separation rate to increase significantly, and thus the electrode can be used as an effective electrode for the water splitting reaction. The over potential required for this electrode to generate a current density of 10 $mAcm^{-2}$ for HER was 110 mV and for an OER of 210 mV. Also, the electrode was used as

Table 2
Electrocatalytic performance of different nanocones structure.

Catalyst	Type of nanostructure	HER activity	OER activity	Overall water splitting	b (mV/dec)	Ref
Ni-CNT	Nanocones	η_{10} = 83 mV η_{20} = 107 mV η_{100} = 206 mV			HER = 55	[96]
Ni-Co Alloy	Nanocones	η_{10} = 107 mV η_{20} = 142 mV η_{100} = 198 mV			HER = 119	[20]
Ni-Cu Alloy	Cone shape	η_{10} = 200 mV η_{20} = 230 mV η_{100} = 310 mV			HER = 82	[97]
Ni-Fe-Co Alloy	Nanocones	η_{10} = 91 mV η_{20} = 119 mV η_{100} = 175 mV	η_{10} = 316 mV η_{20} = 340 mV η_{100} = 375 mV	i_{10} = 1.60 V	HER = 86 OER = 43	[98]
Ni-Co-P	Nanocones	η_{10} = 51 mV η_{20} = 71 mV η_{100} = 110 mV	η_{10} = 221 mV η_{20} = 236 mV η_{100} = 254 mV	i_{10} = 1.53 V	HER = 55 OER = 54	[53]

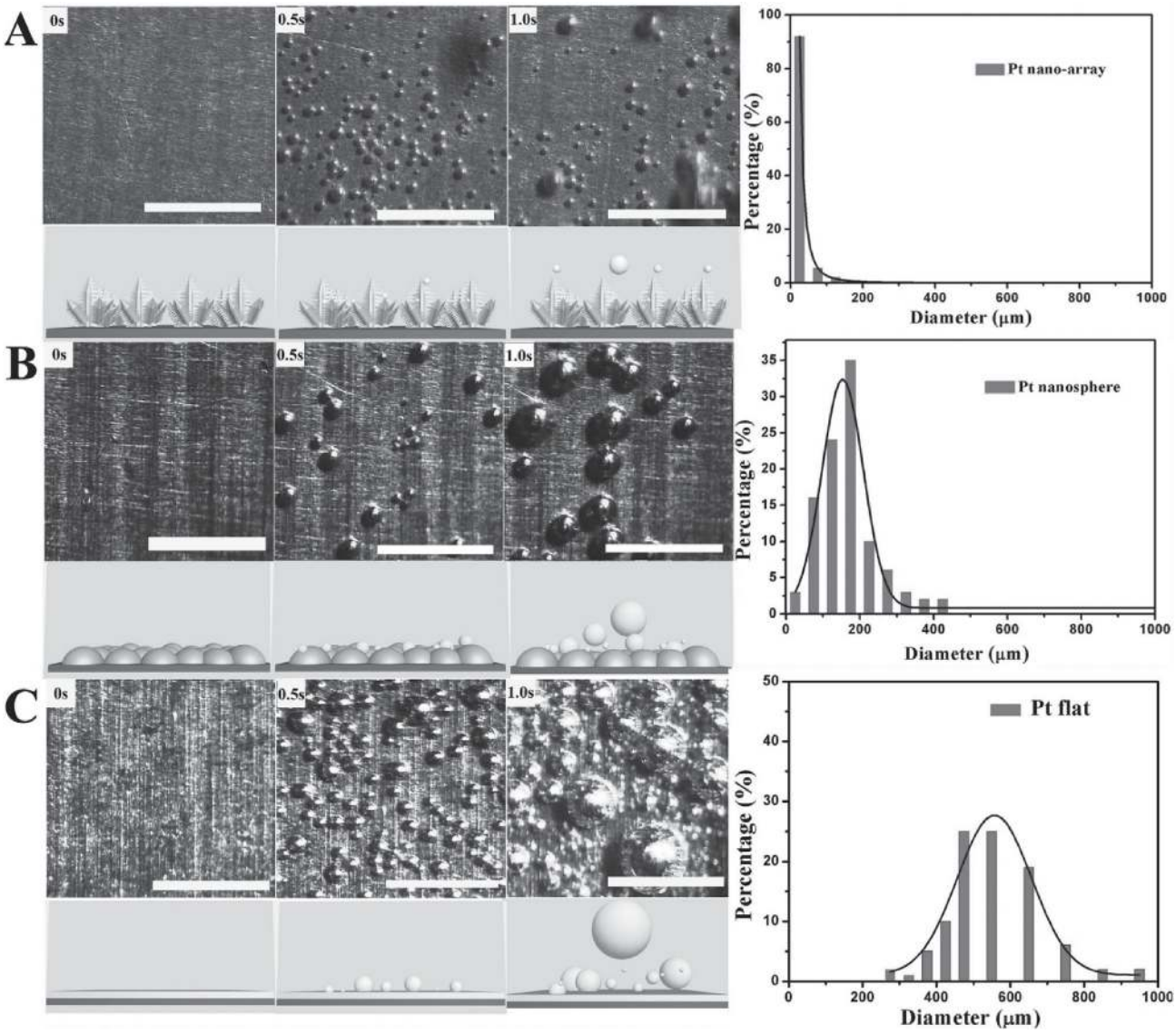

Fig. 9. Digital images show different bubbles and bubble size distribution for each of the structures A) Platinum nanostructure B) Platinum nanosheets and C) Flat film [78].

a bifunctional electrode for HER and OER reactions, requiring 1.56 V to generate a current density of 10 $mAcm^{-2}$.

Increase in the rate of separation of hydrogen and oxygen bubbles during the electrolysis of water carried out by Zhu et al. [70] has also been accomplished through the creation of superaerophobic surfaces. In their study, Ni-Mo nanostructures and Ni-Fe LDH were employed for HER and OER, respectively. The results of electrocatalytic studies indicated that the formation of nanostructured surfaces could significantly improve electrocatalytic activity. The improvement of electrocatalytic activity was attributed to the superaerophobic surface structure, followed by the rapid separation of gas bubbles formed on the surface. These type of nanostructures possess a discontinuous three-phase contact line, which considerably reduces the adhesion force to gas bubbles. It was revealed that Ni-Mo and Ni-Fe LDH adhesion strength is below the identification line, while Pt/C and IrO_2/C electrons exhibit more adhesion. This difference in adhesion force is related to surface morphology. Superaerophobic morphology on Ni-Mo and Ni-Fe LDH electrodes leads to a decrease in adhesion force, as well as an increase in the rate of separation of bubbles on the surface. Furthermore, the distribution of bubbles size on the surface also indicates that the nanostructured surface reduces the distribution of the diameter of the bubbles on the surface. All observations show that the creation of superaerophobic surfaces leads to a rapid increase in the separation of bubbles from the surface of the electrode, thereby increasing the electrocatalytic activity.

Hao et al. [76] developed ultrafine superaerophobic and superhydrophilic Cu_3P microplates using phosphidated microscopic copper plates on nickel foam and investigated their electrocatalytic properties for HER and OER. They showed that superhydrophobicity and superaerophobicity of these microplates result in a better penetration process at the electrode-electrolyte interface and faster separation of gas bubbles from the surface of the electrocatalyst. Microplates were produced at various temperatures, whereas the microspheres produced at 450 °C exhibited excellent electrocatalytic properties for OER and HER, in which 290 mV and 130 mV overpotentials were required for HER and OER to generate a current of 10 $mAcm^{-2}$. The reason for this was investigated in the amount of wettability. The underwater bubble contact angle for microplates produced at 450 °C is 155.7°, which is greater than the other values. This leads to the rapid separation of the bubbles from the surface and improves the electrocatalytic properties. Moreover, digital images of the bubbles formed on the three surfaces are shown that the bubbles have not accumulated on the surface of the

electrode formed at 450 °C, which is due to the improvement of the permeation process and the rapid separation of bubbles from the surface.

The other process during the water electrolysis reaction in which bubbles are produced is the OER. In general, for the creation of an electrode with high electrocatalytic activity for OER, it is necessary to select an active catalyst and superaerophobic. The Ni_2Co_1@$Ni_2Co_1O_x$ catalyst with superaerophobicity properties was created by He et al. [105]. In the first stage, the Ni_2Co_1@ $Ni_2Co_1O_x$ catalyst was first created by the resuscitation of $Ni_2Co_1O_4$ nanowires under the ammonia atmosphere, resulting in the formation of Ni_2Co_1@ $Ni_2Co_1O_x$. Afterwards, Ni_2Co_1@$Ni_2Co_1O_x$/Nafion was created by coating a mixture of Ni_2Co_1@$Ni_2Co_1O_x$ and Nafion polymer on nickel plates Later, the Ni_2Co_1@$Ni_2Co_1O_x$ superaerophobic electrode was digested with air Ni_2Co_1@$Ni_2Co_1O_x$/Nafion and NH_3 gas to isolate the Nafion hydrophobic polymer and minor restitution of $Ni_2Co_1O_x$. The resulting electrode exhibited negligible separation force for oxygen gases. The creation of this electrode has been very effective in increasing the number of active sites for OER reactions. Furthermore, the superaerophobic state created rapidly separates the oxygen bubbles from the surface and thereby improves electrocatalytic activity.

Tungsten carbide is one of the essential electrocatalytic materials for HER, but slow separation rates of hydrogen bubbles and the formation of high bubble resistance hinders electrocatalytic properties. For this purpose, Han et al. [106] developed nanoarrays of nitrogen-doped tungsten carbide and investigated their electrocatalytic properties for HER and OER. In this study, the doping of nitrogen led to the creation of an optimal energy state for optimizing the hydrogen bond, thus improving the kinetics of HER and creating nanoarrays not only resulting in increased active surface area but also leading to the creation of a superaerophobic surface and consequently, increased bubbles separation rate. LSV curves for different electrodes of this study are shown in Fig. 10a and the separation behavior of bubbles on the surface of these electrodes is also represented in Fig. 10b. The surface nanostructuring and the doping of nitrogen have led to better electrocatalytic properties, where the optimal sample requires 89 mV overpotential to generate a current density of 10 mA cm^{-2}. The enhanced electrocatalytic activity can be attributed to surface nanostructures and nitrogen doping. The separation behavior of the bubbles shows that the bubbles are removed more rapidly from the surface on the nanostructures and that the size of the bubbles is smaller on these surfaces. These results indicate that the adhesion of the bubbles to the nanostructure is weaker than on other surfaces. Adhesion of bubbles on a surface can be assessed by the adhesion force and the contact angle. The contact angle on the non-nanostructured surface (N-WC) was 148° and the adhesion force was equal to 12 μN, whereas the contact angle was 163° for the nanoscale surface (N-WC nanoarrays) and adhesion force was calculated roughly equal to zero. These results emphasize that surface roughness improves electrocatalytic activity by weakening the reactions between bubbles with electrodes.

The use of superaerophobic surfaces to improve the electrocatalytic behavior of LDHs has been reported by Haoyi et al. [107]. In their study, hybrid nanotubes (FeCoNi-HNTAs) were created and their electrocatalytic properties were investigated. The synthesized electrodes exhibited excellent electrocatalytic properties and required an overpotential of 58 mV to generate a current density of 10 mA cm^{-2} for HER and 184 mV for OER. One of the most important reasons for the desirable electrocatalytic properties achieved in this study was improving the behavior of hydrogen bubble separation by creating a nanostructured surface. Bubble separation behavior was evaluated by measuring the underwater contact angle, as well as measuring the adhesion force. It can be found that there is no adhesion between the bubbles and the electrode surface for the FeCoNi-HNTAs electrode. In addition, the bubble contact angle for this electrode was measured at 171°, which indicates the superaerophobicity of the electrode. This can be attributed to the non-continuous three-phase contact line bubble with the surface of this electrode. The continuous TPCL renders the contact between the bubbles and the surface of the electrode negligible, and therefore the adhesive force between the bubble and the surface of the electrode is reduced.

Also, graphene base compounds can also be created as a superaerophobic surface, in which case the excellent electrocatalytic activity and stability de could be expected. Vertical graphene nanohills, which are capable of good separation of hydrogen bubbles [108]. In order to improve the inherent electrocatalytic properties, graphene surface was covered by WS_2 nanoparticles. Compared to the smooth surface of this nanostructure, its superaerophobic surface exhibited excellent electrocatalytic properties, with an onset potential of 36 mV. This is while the onset potential of the flat surface was reported at 288 mV. Distribution of bubble sizes on a flat surface and on the superaerophobic surface is shown in Fig. 11. These results clearly indicate that the size of the bubbles separated from the surface of the nanostructured electrode is much smaller than that of the flat surface, which results in lower bubble resistance. Finally, in order to compare the electrocatalytic behavior of the various electrodes studied in this review article, the electrocatalytic activity of these electrodes is summarized in Table 3.

Different types of nanostructures were investigated to improve the bubble separation of the anode and cathode during electrochemical water splitting. Since the electrodes used to create these nanostructures are different, and since electrocatalytic activity depends on the active

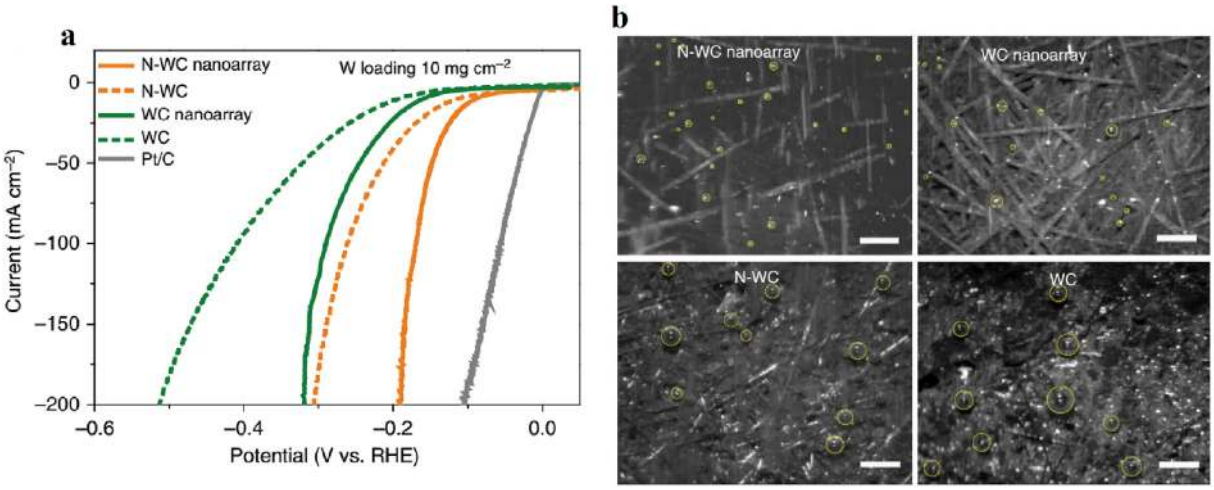

Fig. 10. a) LSV curves of different electrodes and b) bubbles separation behavior images on the different electrodes [106].

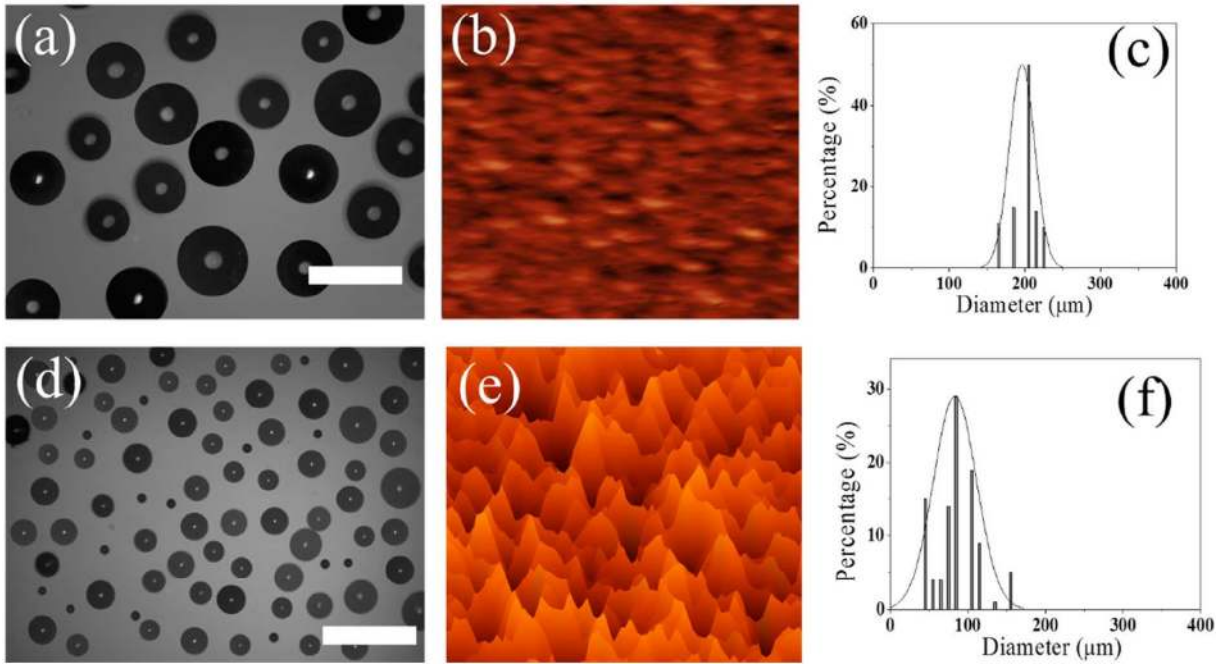

Fig. 11. The images represent the size of the hydrogen bubbles created on the electrode surface during the HER reaction. a) for a smooth surface and d) for a nanostructure surface [108].

surface area and the inherent electrocatalytic activity, it is generally not possible in this case to exactly study the influence of the types of nanostructures to improve the separation of the bubble from the surface and thus improving the electrocatalytic activity. Therefore, it can be said that the effect of various roughness regimes on the bubble separation from the surface is ambiguous and complete and comprehensive study on the effect of different types of nanostructures on the separation of the bubble from the surface is needed. In order to achieve this goal, it is necessary to consider the same material in order to have same intrinsic activity.

4.1.3. Limitation of superaerophobic surfaces

Besides all the advantages that have been noted for the superaerophobic surface in the previous sections for the rapid increase of bubbles from the surface, and as a result of the improvement of electrocatalytic activity, these surfaces also have disadvantages and limitations. One of the main constraints of these surfaces is their construction and synthesis methods. In most cases, the construction and synthesis of these surfaces in order to reach nanostructure surfaces are very difficult, long and costly. On the other hand, the other disadvantages of these levels are the limitations of creating these levels for all active substances. All materials cannot be obtained in the nanostructured form, and as a result, much research is needed to develop methods for fabricating the active materials with easy methods. Also, research on the creation of superaerophobic surfaces is still in its early stages, and many studies are needed to formulate the variables of superaerophobic surfaces.

4.2. Usage of magnetic fields

The process of separating the bubbles from the surface of the electrode is a common phenomenon of mass transfer. Bubble growth is controlled by common phenomena in a three-phase region where bubbles, electrolytes, and electrode surfaces interact. With time, the released hydrogen accumulates on the electrode surface and forms a supersaturated layer. Hydrogen is transmitted through the penetration and convection of the electrode surface. Therefore, management of the bubbles on the surface of the electrocatalyst is one of the crucial issues in the electrolysis of water and has subsequently attracted a great deal of attention in recent years. A series of studies have indicated that the magnetic field has a significant effect on the process of bubble separation during water electrolysis [112,113]. This research has revealed that bubble-covered fraction, as well as the size of the bubbles, decrease with the application of the external magnetic field. Furthermore, the water electrolysis process and the ohmic drop between the electrodes is decreased as a result of the application of the magnetic field [114]. Reducing the bubble-covered fraction on the surface, lowering the size of bubbles on the surface while increasing the efficiency

Table 3
Electrocatalytic performance of other nanostructure for improving bubble detachment during water splitting.

Catalyst	Type of nanostructure	HER activity	OER activity	Overall water splitting	b (mV/dec)	Ref
FeNi LDH@NWSSF	Nano woven	η_{10} = 110 mV	η_{10} = 210 mV		HER = 113 OER = 56	[104]
Nitrogen-doped tungsten carbide	Nanowire	η_{10} = 113 mV	η_{60} = 470 mV		HER = 75	[106]
FeCoNi-HNTAs	nanotube	η_{10} = 58 mV	η_{10} = 184 mV	i_{10} = 1.429 V	HER = 37.5 OER = 49.9	[107]
VGNHs-WS_2	nanohills	Onset = 36 mV			HER = 162	[108]
Ni_2P	Nanoarray	η_{10} = 35 mV				[109]
Nickel-Cobalt Hydroxide	Nano dendrite		η_{10} = 225 mV			[110]
NiS-Ni_2P	Nanoflake-nanoparticles	η_{10} = 103 mV			HER = 68	[111]

of the water electrolysis under the influence of the external magnetic field are in fact ascribed to the Lorentz-force-driven convection. The external magnetic field results in the application of magnetohydrodynamic (MHD) convection, which leads to the application of excess convection on the electrolyte, effectively reducing the harmful effects of bubble accumulation on the surface [115].

The Lorentz force is applied to the moving charged particles in an electric-magnetic field, which is expressed as follows [116]:

$$F = qE + qv \times B \quad (26)$$

In which F is the Lorentz force, q is the particle charge, E is the electric field intensity, B is the density of the flux of the magnetic field and v is the particle velocity.

Multiple studies have been carried out on the usage of a magnetic field to reduce the harmful effects of bubbles during the water electrolysis. Koza et al. [112] examined the effect of uniform magnetic field on the HER during electrolysis of water in 0.1 M $NaSO_4$ solution. In their study, electrochemical techniques and microscopic studies were utilized to evaluate the effect of the magnetic field on the separation behavior of hydrogen bubbles. Images of the size of the bubbles on the electrode surface during the water electrolysis reaction in the absence and presence of a magnetic field (70 mT) are shown in Fig. 12 It is observed that in presence of a magnetic field, the size of the bubbles is decreased and that the distribution of bubble sizes in the presence of a magnetic field becomes narrower (Fig. 12 f). In the absence of a magnetic field, however, the size of the bubbles during the separation is 600 μm. By applying the magnetic field, the size of the bubbles is lowered by 400 μm during separation. These results are also shown by other researchers and agree with their findings [55,117]. The reason for reducing the bubble size caused by the magnetic field can be described as in electromagnetic filed in parallel with the electrode surface, the electrical and magnetic fields are perpendicular to each other which leads to the macroscopic convection caused by the Lorentz force [118]. The bubbles on the surface of the electrode act as a barrier and a hydrodynamic drag will be created over the bubble. This leads to a decrease in the size of the bubble on the surface and the rapid separation of the bubble from the surface, and as a result, depolarization takes place [119]. Also, bubble combinations, which are important in the separation of bubbles, are also improved. A schematic of the phenomena above is presented in Fig. 13.

In another study, Lin et al. [114] investigated the effects of the magnetic field on the hydrogen production in the water electrolysis. The images of the separation of bubbles from the electrode surface in the presence and absence of a magnetic field are shown in Fig. 14. In Fig. 14a, the motion of the bubbles is shown when the Lorentz force is upward. When the time is less than 1/3 s, the bubbles are generated on the surface of the electrode, whereas when the time is between 1/3 and 2/3 s, more bubbles are formed on the left electrode surface in comparison to that of the right. The bubbles formed on the left side are hydrogen, while the bubbles created on the right side are oxygen. In Fig. 14b, the separation behavior of bubbles is shown in the absence of a magnetic field. The direction of the gas bubbles does not tend to a certain direction and they are in the vertical direction. This means that the movement of the bubbles in the water electrolysis does not deviate in the absence of a magnetic field and that the magnetic field will affect the convection of the electrolyte. It is also shown in Fig. 14c that by turning the Lorentz force downward, gas bubbles also move downward. Possible forces in the shape near the electrode surface are shown in Fig. 14 d and e. In Fig. 14d, Lorentz force is in a downward direction. Although the buoyancy force is upward, the bubbles may move downward due to the Lorentz force. In Fig. 14e, the Lorentz force acts in an upward direction. Because both Lorentz force and buoyancy forces are upward, hydrogen bubbles can be removed from the electrode region faster than they are generated, resulting in lower electrochemical polarization. The negative and positive Lorentz force is an important criterion in improving efficiency during the water electrolysis process. Therefore, it can be seen that the flow fields of hydrogen and oxygen during the water electrolysis are a function of magnetic force direction. When the buoyancy forces of hydrogen and Lorentz force are upward, the convection caused by the Lorentz force improves the separation of the bubbles, and thus the efficiency of the hydrogen production is improved. Conversely, if these two forces are in the opposite direction, the production of hydrogen will be hindered. Therefore, it can be concluded that the magnetic force in the correct direction can play an important role in improving the efficiency of hydrogen production. In addition, Elias et al. [120] examined the effect of the magnetic field on the Ni-W coating electrocatalytic activity. In their study, the intensity of the magnetic field varied from 0.1T to 0.4 T. The results indicated that electrocatalytic activity is enhanced with the application of a magnetic field. With the increase in the magnetic field from 0.1 T to 0.4 T, the amount of produced hydrogen bubble was increased from 16.4 to 19.1 cm^3 during 300 s. The reason for improved catalytic activity is magnetohydrodynamic (MHD) power-induced convection and rapid separation of hydrogen bubbles.

4.3. Usage of ultrasonic fields

The ultrasonic field is one of the most powerful fields for increasing the charge transfer and improving the efficiency of electrochemical reactions, which is due to the influence of cavitation. In general, water electrolysis is affected by the surface covered with gas bubbles and the dispersion of bubbles from the surface. Therefore, improving the electrolysis efficiency of water is influenced by the control of these parameters. Since the generated gas bubbles on the electrode surface are related to common-sector phenomena in the three-phase region, the three-phase boundary layer needs to be disintegrated in order to improve the water electrolysis. Therefore, ultrasonic fields can be used for quick removal of bubbles from the surface of the electrodes. Using ultrasonic fields to improve the electrolysis efficiency of water is very cost effective. Since the cost spent to create an ultrasonic field is negligible compared to the conserved energy. For example, in a cell with 100 Ka, the amount of generated overpotential as a result of bubbles is about 0.3 V. The conserved energy through the removal of this overpotential by applying a magnetic field is about 30 kW. However, the amount of energy needed to create this ultrasonic field is about 0.05 kW. Regarding the usage of ultrasonic fields to improve the electrolysis efficiency, Sheng-De Li et al. [121] used ultrasonic fields to enhance HER and OER response. Water electrolysis reaction was performed at different concentrations of solution. First of all, it is observed that by increasing the concentration of the solution, the electrocatalytic properties are improved, which is due to the decrease in the amount of solution resistance. It can also be seen that with the application of the ultrasonic field, the cell voltage is lowered and the electrocatalytic properties of the HER and OER are further improved. By applying the ultrasonic field to the electrochemical phenomena of a common area that occurs in the three-phase area of the bubble, the electrolyte of the layer of volume, the surface area of the electrochemical reactions is increased due to the rapid separation of the bubbles from the surface. Moreover, the efficiency of hydrogen gas production is increased by about 18.5% through the application of the magnetic field. Furthermore, the amount of the conserved energy is increased by about 10–25% applying the ultrasonic field.

4.4. Usage of supergravity fields

One of the other methods of improving the separation of bubbles from the surface of the electrode during the water electrolysis is using supergravity fields. During the phase separation, fluid dynamics behavior is controlled by the term interphase buoyancy. In gas/liquid systems, heavy phases (i.e. electrolytes) move in the direction of gravitational acceleration, while light phases (i.e. bubbles) move in the opposite direction (i.e. in the direction of buoyancy). If HER process can

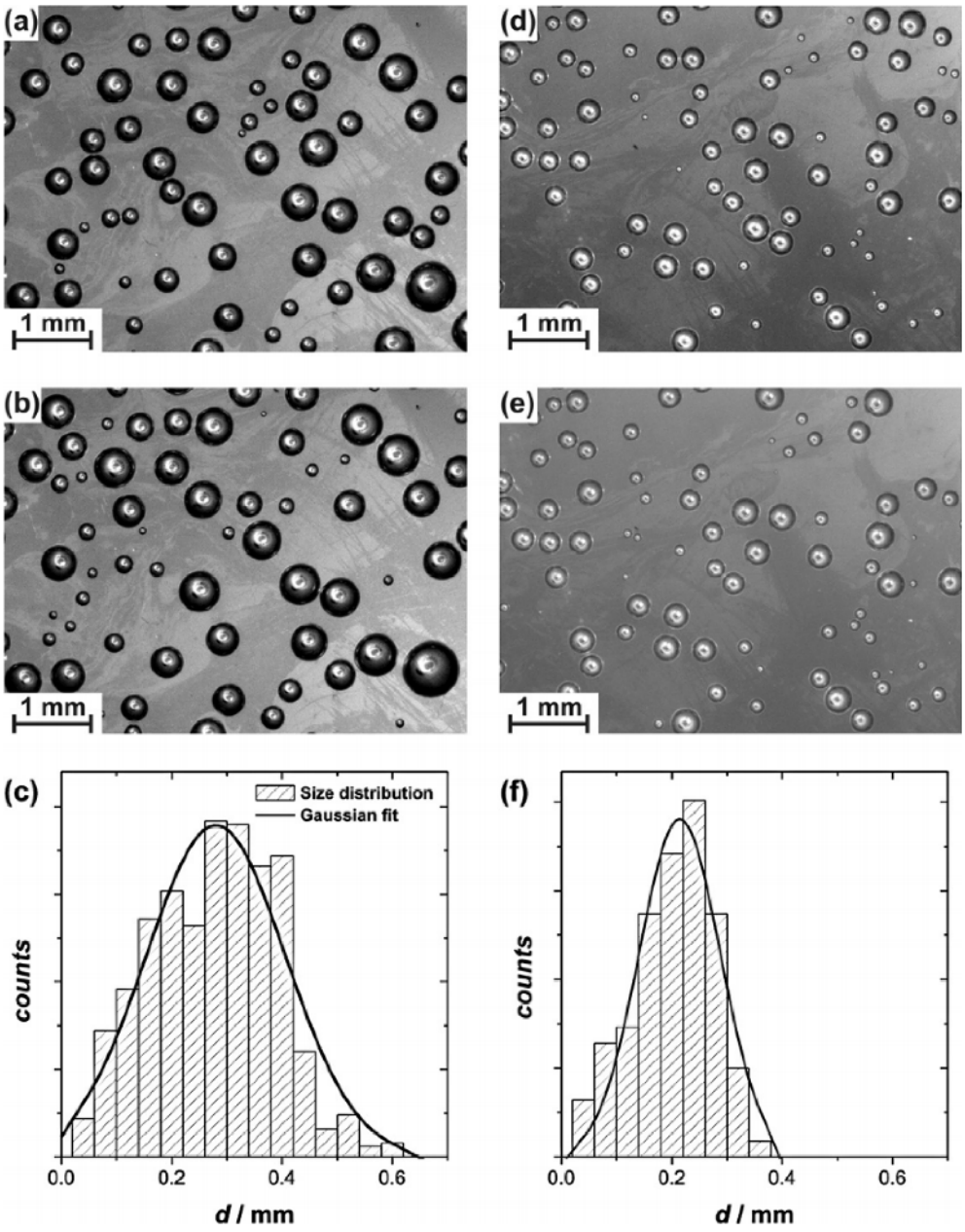

Fig. 12. Hydrogen bubbles formed on the surface of the electrode in the absence of a) and b) in the presence of an external magnetic field equal to 70 mT (d and e); and c) distribution of bubble sizes on the surface in the absence of a magnetic field; and f) the distribution of size of the bubbles on the surface in the presence of a magnetic field [112].

be influenced by the supergravity field, the gravitational acceleration environment can be strengthened, resulting in an increased rate of separation of bubbles from the surface of the electrode. Therefore, the bubble layer on the surface can be increased by using supergravity fields, consequently improving the electrocatalytic properties [122]. Recently, a great deal of research has been carried out on the use of supergravity fields for removal of bubbles from the surface [123–125]. All of these studies have proven that by using a supergravity field, the gas-producing reaction can be improved, and as a result, reduce the amount of cell potential. Wang et al. [122] accurately investigated how HER was affected by supergravity field. In their study, HER was performed in different magnitudes of supergravity fields., It was observed that by increasing the magnitude of the field, the amount of potential required for the creation of a flow rate is reduced, which results in an improvement in the electrocatalytic properties of hydrogen production. With regards to the LSV curves, it can be seen that with increasing the current density, the impact of the supergravity field is increased further.

During the HER process influenced by a supergravity field, higher amounts of supergravity fields lead to a decrease in the critical radius of the bubble formation. Moreover, it can be concluded that the separation of the bubble from the surface of the electrode is mainly affected by the buoyancy force, which causes the radius of the formed bubble on the surface to be under the influence of the supergravity field. Also, when HER is in normal gravitational conditions, the bubbles are created perpendicularly along the surface of the electrode, and the separation of the bubbles from the electrode surface takes place from the common interface line between the bubble and the electrode surface (Fig. 15A) whereas the separation of bubbles from the surface of the electrode takes place according to Fig. 15B when under the influence of the supergravity field. It can be concluded that under the influence of the supergravity field, the contact time between the bubble and the electrode surface is decreased, which results in the electrocatalytic

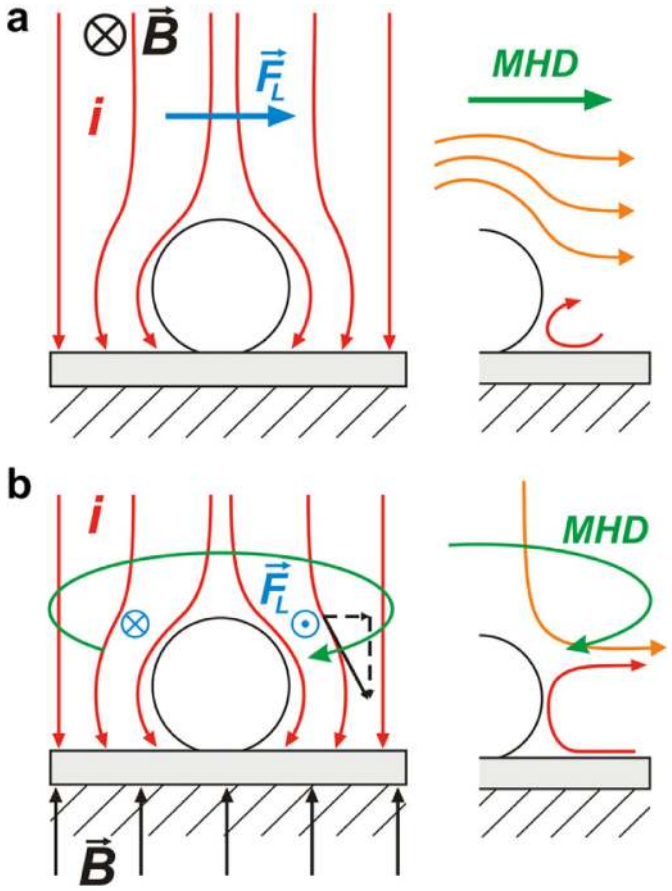

Fig. 13. Schematic of current distribution along with Lorentz force (left) and characteristic convection patterns (right) near the bubble created in parallel (a) and perpendicular to (b) magnetic field [112].

properties being improved [123].

In addition, Mat et al. [126] have shown that the separation rate of gas bubbles with a low radius from the surface of the electrode is increased with the application of supergravity field. High buoyancy force and lower volume of bubbles under the supergravity field are useful for rapid separation of bubbles. As a result, the thickness of the substrate is decreased near the surface of the electrode under the supergravity field in comparison to the gravitational field, which reduces the effect of bubbles.

Studies have shown that the relationship between the voltage of the cell under the supergravity field and gravity coefficient is defined as follows [127,128]:

$$U_G = D \log_G + U_1 \quad (27)$$

In which U_1 is the voltage of the cell under normal gravity conditions, and D is a negative constant at any given current density. The results indicate that the effect of supergravity field on decreasing the voltage value of the cell is increased in proportion with current density. In addition, it has been shown that the decrease in the bubble effect has a greater contribution to the decrease of overpotential reactions in lowering the voltage of the cells, which this effect tends to increase at higher current densities.

As was discussed above, it is revealed that the use of foreign fields reduces the effect of bubbles, thereby improving the performance of electrolysis cells of the water. However, the cost and the energy needed to create these fields should also be taken into consideration and compared with the cost of reducing the potential of water splitting. For instance, the energy required to create a magnetic field or supergravity field should be smaller than the conserved energy of the water electrolysis reaction, so that the use of these fields for reducing the effect of the bubble would have an economic justification. Cheng et al. [127] estimate that at a current value of 100 Ka and 2 kW to create supergravity, roughly 30 kW of energy is conserved.

4.5. Limitation of different fields

It has been seen in previous sections that the use of different fields leads to rapid separation of bubbles from the surface in small sizes and thus leads to an improvement in the electrocatalytic activity. However, these fields also have disadvantages and limitations. One of the main constraints of these fields is the limitation of the use of industrial scale due to the high cost of applying these fields. So, the magnetic, supergravity and ultrasonic fields are not cost-effective for industrial hydrogen production and more investigation is needed for being industrial application of these fields. Superhydrophobic surfaces can be fabricated by some active compounds and can be employed for industrial application.

5. Conclusion, challenges and future trend

In this review, recent advances in the methods and technologies for improving the separation of hydrogen and oxygen bubbles are summarized from cathode and anode surfaces, respectively. Initially, the importance of the development of hydrogen electrocatalysts and harmful effects of bubbles in the decrease of electrocatalytic activity was pointed out. In general, methods of improving the bubble separation from the surface include fabrication of superaerophobic surfaces and usage of magnetic, supergravity and ultrasonic fields. Superaerophobic surfaces, result in smaller bubble sizes and rapid separation of bubbles from the surface through disassembly of TPLC, effectively improving the separation of bubbles from the surface which results in improving electrocatalytic activity and stability trough decreasing in adhesion force applied from the bubble to the electrode surface. Usage of these fields reduces the covered area by bubbles by application of magnetohydrodynamic (MHD) convection, which in turn lowers the harmful effect of bubbles and improves electrocatalytic activity. As we have seen, one of the most important methods for reducing the bubble resistance is the design of a microstructure in such a way as to create an superaerophobic surface. Based on the works reviewed in this article, we can provide suggestions for future studies and research paths in this research field as follows. In general, a noble metallic electrode shows the best electrocatalytic properties. If in order to reduce the negative effect of the bubble, these electrodes can be created in the form of nanostructures on the surface, then an extremely high electrochemical kinetics can be obtained, resulting in an excellent electrocatalytic activity. Also, in order to reduce costs and create an affordable electrode as well as to reduce the resistance created by the bubble, a noble catalyst can be deposited on the surface of the prepared nanoarrays as nanoparticles and achieve excellent electrocatalytic properties. So, one of the important research areas in the future can be the design of new nanostructures with simple and cost-effective methods to reduce bubble resistance. Also, if it is possible to simultaneously improve the inherent electrocatalytic activity of certain nanostructures, an electrode with excellent electrocatalytic activity can be achieved. Accordingly, for future studies, it is suggested that a variety of electrocatalysts with high intrinsic activity be created in three-dimensional arrays in order to minimize the negative effects of hydrogen and oxygen bubbles. Accordingly, the synthesis of electrodes, a) metal doped hydroxide, b) metal oxides, metal phosphides, metal and carbon selenides in the 3-dimensional state is proposed. Besides, in order to further enhance the activity and stability, the synthesis of these electrodes is proposed as binder-free, in which binders are not used in the fabrication of these electrodes.

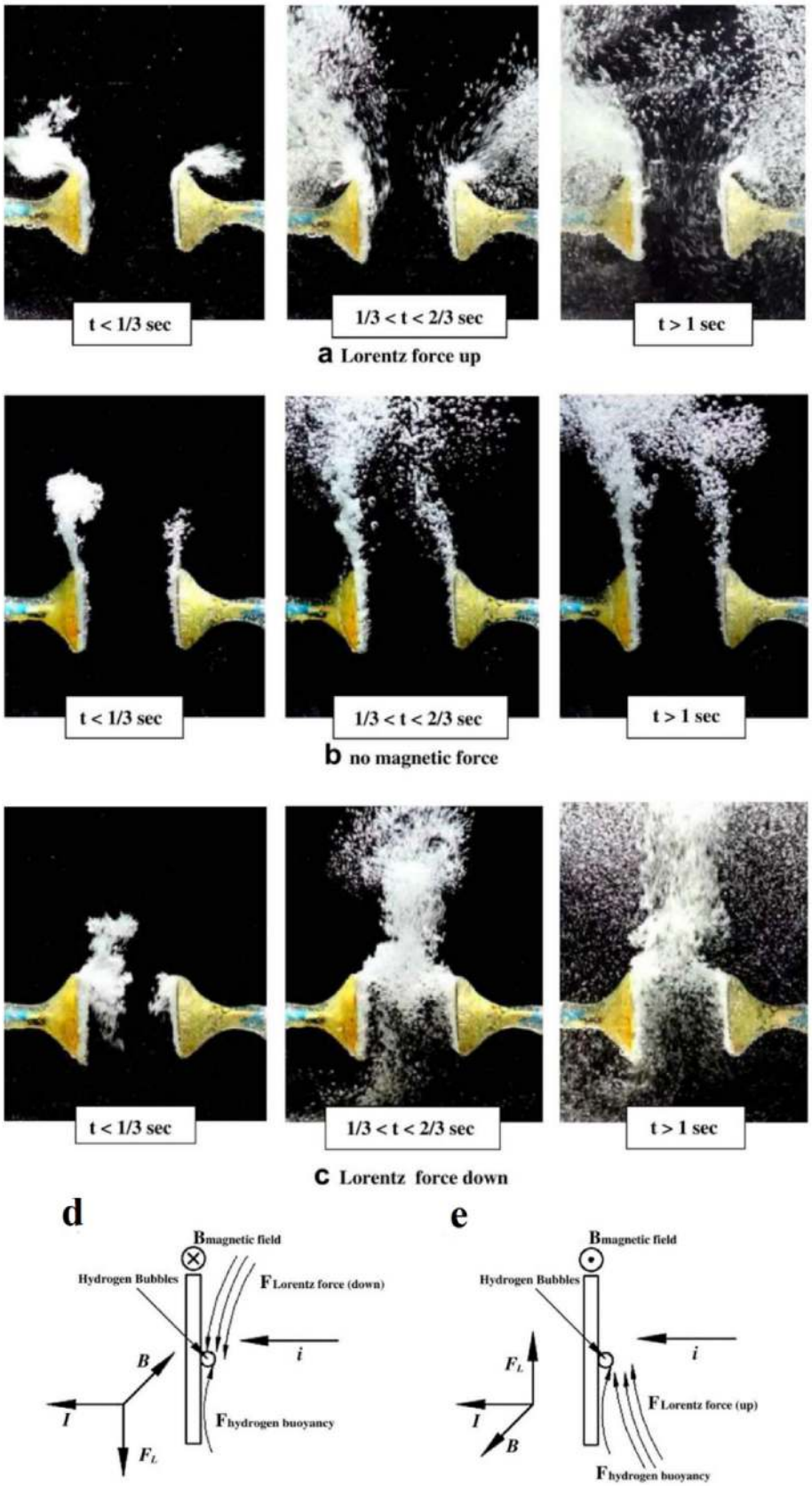

Fig. 14. The convective phenomenon for different magnetic directions. (Voltage: 4 V, electrode distance: 10 mm, KOH: wt 40%, magnetic strength: 4.5 T) [114].

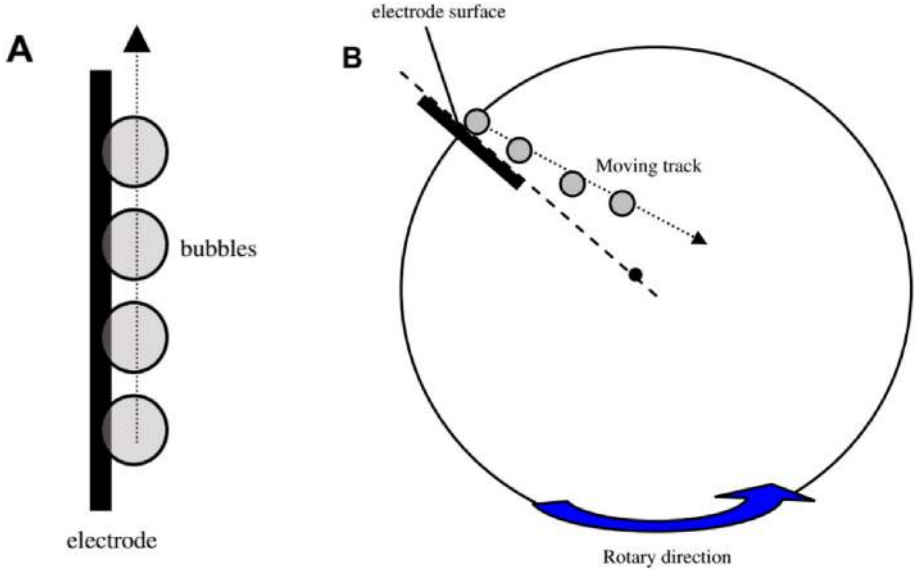

Fig. 15. The direction of moving the bubbles from the surface of the electrode into the electrolyte in A) is the normal gravity condition and B) under the influence of the super gravity field [122].

Acknowledgements

A part of this work was financially supported by the DGIST R&D Program of the Ministry of Science, ICT and Future Planning of Korea (19-IT-02).

References

[1] Zhang R, Russo PA, Feist M, Amsalem P, Koch N, Pinna N. Synthesis of nickel phosphide electrocatalysts from hybrid metal phosphonates. ACS Appl Mater Interfaces 2017;9:14013–22.
[2] Jiang P, Liu Q, Ge C, Cui W, Pu Z, Asiri AM, et al. CoP nanostructures with different morphologies: synthesis, characterization and a study of their electrocatalytic performance toward the hydrogen evolution reaction. J Mater Chem 2014;2:14634–40.
[3] Wang X-D, Xu Y-F, Rao H-S, Xu W-J, Chen H-Y, Zhang W-X, et al. Novel porous molybdenum tungsten phosphide hybrid nanosheets on carbon cloth for efficient hydrogen evolution. Energy Environ Sci 2016;9:1468–75.
[4] Tian J, Liu Q, Liang Y, Xing Z, Asiri AM, Sun X. FeP nanoparticles film grown on carbon cloth: an ultrahighly active 3D hydrogen evolution cathode in both acidic and neutral solutions. ACS Appl Mater Interfaces 2014;6:20579–84.
[5] Wang X, Liu R, Zhang Y, Zeng L, Liu A. Hierarchical Ni 3 S 2-NiOOH hetero-nanocomposite grown on nickel foam as a noble-metal-free electrocatalyst for hydrogen evolution reaction in alkaline electrolyte. Appl Surf Sci 2018;456:164–73.
[6] Zhang L, Li S, Gomez-Garcia CJ, Ma H, Zhang C, Pang H, et al. Two novel polyoxometalate-encapsulated metal-organic nanotube frameworks as stable and highly efficient electrocatalysts for hydrogen evolution reaction. ACS Appl Mater Interfaces 2018;10(37):31498–504.
[7] Darband GB, Aliofkhazraei M, Rouhaghdam AS. Nickel nanocones as efficient and stable catalyst for electrochemical hydrogen evolution reaction. Int J Hydrogen Energy 2017;42:14560–5.
[8] Ji Y, Yang L, Ren X, Cui G, Xiong X, Sun X. Nanoporous CoP3 nanowire array: acid etching preparation and application as a highly active electrocatalyst for the hydrogen evolution reaction in alkaline solution. ACS Sustainable Chem Eng 2018;6:11186–9.
[9] Rezaei B, Jahromi ART, Ensafi AA. Porous magnetic iron-manganese oxide nanocubes derived from metal organic framework deposited on reduced graphene oxide nanoflake as a bi-functional electrocatalyst for hydrogen evolution and oxygen reduction reaction. Electrochim Acta 2018;283:1359–65.
[10] Manabe A, Kashiwase M, Hashimoto T, Hayashida T, Kato A, Hirao K, et al. Basic study of alkaline water electrolysis. Electrochim Acta 2013;100:249–56.
[11] Kuai L, Geng J, Chen C, Kan E, Liu Y, Wang Q, et al. A reliable aerosol--spray-assisted approach to produce and optimize amorphous metal oxide catalysts for electrochemical water splitting. Angew Chem 2014;126:7677–81.
[12] Lv X, Zhu Y, Jiang H, Yang X, Liu Y, Su Y, et al. Hollow mesoporous NiCo 2 O 4 nanocages as efficient electrocatalysts for oxygen evolution reaction. Dalton Trans 2015;44:4148–54.
[13] Tang C, Cheng N, Pu Z, Xing W, Sun X. NiSe nanowire film supported on nickel foam: an efficient and stable 3D bifunctional electrode for full water splitting. Angew Chem 2015;127:9483–7.
[14] Zeng K, Zhang D. Recent progress in alkaline water electrolysis for hydrogen production and applications. Prog Energy Combust Sci 2010;36:307–26.
[15] Yu J, Li Q, Li Y, Xu CY, Zhen L, Dravid VP, et al. Ternary metal phosphide with triple-layered structure as a low-cost and efficient electrocatalyst for bifunctional water splitting. Adv Funct Mater 2016;26:7644–51.
[16] Kosmala T, Coy Diaz H, Komsa HP, Ma Y, Krasheninnikov AV, Batzill M, et al. Metallic twin boundaries boost the hydrogen evolution reaction on the basal plane of molybdenum selenotellurides. Adv. Energy Mater. 2018:1800031.
[17] Wang C, Wang T, Liu J, Zhou Y, Yu D, Chang J-K, et al. Facile synthesis of silk-cocoon S-rich cobalt polysulfide as an efficient catalyst for hydrogen evolution reaction. Energy Environ Sci 2018;11(9):2467–75.
[18] Yang C, Gao MY, Zhang QB, Zeng JR, Li XT, Abbott AP. In-situ activation of self-supported 3D hierarchically porous Ni3S2 films grown on nanoporous copper as excellent pH-universal electrocatalysts for hydrogen evolution reaction. Nano Energy 2017;36:85–94.
[19] Ouyang C, Wang X, Wang C, Zhang X, Wu J, Ma Z, et al. Hierarchically porous Ni3S2 nanorod array foam as highly efficient electrocatalyst for hydrogen evolution reaction and oxygen evolution reaction. Electrochim Acta 2015;174:297–301.
[20] Darband GB, Aliofkhazraei M, Rouhaghdam AS, Kiani MA. Three-dimensional Ni-Co alloy hierarchical nanostructure as efficient non-noble-metal electrocatalyst for hydrogen evolution reaction. Appl Surf Sci 2019;465:846–62.
[21] Zhang B, Lui YH, Ni H, Hu S. Bimetallic (FexNi1 − x)2P nanoarrays as exceptionally efficient electrocatalysts for oxygen evolution in alkaline and neutral media. Nano Energy 2017;38:553–60.
[22] Wu G, Chen W, Zheng X, He D, Luo Y, Wang X, et al. Hierarchical Fe-doped NiOx nanotubes assembled from ultrathin nanosheets containing trivalent nickel for oxygen evolution reaction. Nano Energy 2017;38:167–74.
[23] Barati Darband G, Aliofkhazraei M, Sabour Rouhaghdam A. Nickel nanocones as efficient and stable catalyst for electrochemical hydrogen evolution reaction. Int J Hydrogen Energy 2017;42:14560–5.
[24] Ma B, Yang Z, Chen Y, Yuan Z. Nickel cobalt phosphide with three-dimensional nanostructure as a highly efficient electrocatalyst for hydrogen evolution reaction in both acidic and alkaline electrolytes. Nano Research 2019;12:375–80.
[25] Dong X, Yan H, Jiao Y, Guo D, Wu A, Yang G, et al. 3D hierarchical V-Ni-based nitride heterostructure as pH-universal electrocatalyst for highly efficient hydrogen evolution reaction. J Mater Chem 2019;7:15823–30.
[26] Chen W-F, Muckerman JT, Fujita E. Recent developments in transition metal carbides and nitrides as hydrogen evolution electrocatalysts. Chem Commun 2013;49:8896–909.
[27] Kim B-J, Fabbri E, Abbott DF, Cheng X, Clark AH, Nachtegaal M, et al. Functional role of Fe-doping in Co-based perovskite oxide catalysts for oxygen evolution reaction. J Am Chem Soc 2019;141:5231–40.
[28] Cao Z, Jiang Z, Li Y, Huang C, Li YF. Metal organic gel derived multi metal oxide as effective electrocatalyst for oxygen evolution reaction. ChemSusChem 2019;12:2480–6.
[29] Lv L, Yang Z, Chen K, Wang C, Xiong Y. 2D layered double hydroxides for oxygen evolution reaction: from fundamental design to application. Adv. Energy Mater. 2019:1803358.
[30] Kuang M, Wang J, Jiang L. Bio-inspired photonic crystals with superwettability. Chem Soc Rev 2016;45:6833–54.
[31] Zhou H, Wang H, Niu H, Gestos A, Wang X, Lin T. Fluoroalkyl silane modified silicone rubber/nanoparticle composite: a super durable, robust superhydrophobic fabric coating. Adv Mater 2012;24:2409–12.
[32] Kinoshita H, Ogasahara A, Fukuda Y, Ohmae N. Superhydrophobic/superhydrophilic micropatterning on a carbon nanotube film using a laser plasma-type

hyperthermal atom beam facility. Carbon 2010;48:4403–8.
[33] Xu L, Jiang Q, Xiao Z, Li X, Huo J, Wang S, et al. Plasma-engraved Co3O4 nanosheets with oxygen vacancies and high surface area for the oxygen evolution reaction. Angew Chem Int Ed 2016;55:5277–81.
[34] Lu Z, Sun M, Xu T, Li Y, Xu W, Chang Z, et al. Superaerophobic electrodes for direct hydrazine fuel cells. Adv Mater 2015;27:2361–6.
[35] Xu H, Ci S, Ding Y, Wang G, Wen Z. Recent advances in precious metal-free bifunctional catalysts for electrochemical conversion systems. J Mater Chem 2019;7:8006–29.
[36] Strmcnik D, Castelli IE, Connell JG, Haering D, Zorko M, Martins P, et al. Electrocatalytic transformation of HF impurity to H 2 and LiF in lithium-ion batteries. Nature Catalysis 2018;1:255.
[37] Wang J, Xu F, Jin H, Chen Y, Wang Y. Non-noble metal-based carbon composites in hydrogen evolution reaction: fundamentals to applications. Adv Mater 2017;29:1605838.
[38] Krstajić N, Popović M, Grgur B, Vojnović M, Šepa D. On the kinetics of the hydrogen evolution reaction on nickel in alkaline solution: Part I. The mechanism. J Electroanal Chem 2001;512:16–26.
[39] Chen L, Lasia A. Study of the kinetics of hydrogen evolution reaction on nickel-zinc powder electrodes. J Electrochem Soc 1992;139:3214–9.
[40] Bockris J, Reddy A, Gamboa-Aldeco M. Modern Electrochemistry 2A, Fundamentals of Electrodics. 2nd ed.Kluwer Academic New York: Plenum Publishers; 2000.
[41] González-Buch C, Herraiz-Cardona I, Ortega E, García-Antón J, Pérez-Herranz V. Synthesis and characterization of macroporous Ni, Co and Ni–Co electrocatalytic deposits for hydrogen evolution reaction in alkaline media. Int J Hydrogen Energy 2013;38:10157–69.
[42] Zheng Y, Jiao Y, Jaroniec M, Qiao SZ. Advancing the electrochemistry of the hydrogen-evolution reaction through combining experiment and theory. Angew Chem Int Ed 2015;54:52–65.
[43] Cai P, Huang J, Chen J, Wen Z. Oxygen-Containing amorphous cobalt sulfide porous nanocubes as high-activity electrocatalysts for the oxygen evolution reaction in an alkaline/neutral medium. Angew Chem Int Ed 2017;56:4858–61.
[44] Trasatti S. Electrocatalysis in the anodic evolution of oxygen and chlorine. Electrochim Acta 1984;29:1503–12.
[45] Razmjooei F, Singh KP, Yang D-S, Cui W, Jang YH, Yu J-S. Fe-treated heteroatom (S/N/B/P)-Doped graphene electrocatalysts for water oxidation. ACS Catal 2017;7:2381–91.
[46] Handoko AD, Deng S, Deng Y, Cheng AWF, Chan KW, Tan HR, et al. Enhanced activity of H 2 O 2-treated copper (II) oxide nanostructures for the electrochemical evolution of oxygen. Catal Sci Technol 2016;6:269–74.
[47] Ghosh S. Fundamentals of Electrical and Electronics Engineering. PHI Learning Pvt. Ltd.; 2007.
[48] Newman J. Electrochemical Systems. Englewood Cliffs, New Jersey: Prentice-Hall; 1991.
[49] Aldas K. Application of a two-phase flow model for hydrogen evolution in an electrochemical cell. Appl Math Comput 2004;154:507–19.
[50] Wang M, Wang Z, Gong X, Guo Z. The intensification technologies to water electrolysis for hydrogen production–A review. Renew Sustain Energy Rev 2014;29:573–88.
[51] George JE, Chidangil S, George SD. Recent progress in fabricating superaerophobic and superaerophilic surfaces. Advanced Materials Interfaces 2017;4:1601088.
[52] Yong J, Chen F, Fang Y, Huo J, Yang Q, Zhang J, et al. Bioinspired design of underwater superaerophobic and superaerophilic surfaces by femtosecond laser ablation for anti-or capturing bubbles. ACS Appl Mater Interfaces 2017;9:39863–71.
[53] Darband GB, Aliofkhazraei M, Hyun S, Rouhaghdam AS, Shanmugam S. Electrodeposited NiCoP hierarchical nanostructure as a cost-effective and durable electrocatalyst with superior activity for bifunctional water splitting. J Power Sources 2019;429:156–67.
[54] Kiuchi D, Matsushima H, Fukunaka Y, Kuribayashi K. Ohmic resistance measurement of bubble froth layer in water electrolysis under microgravity. J Electrochem Soc 2006;153:E138–43.
[55] Gabrielli C, Huet F, Nogueira R. Fluctuations of concentration overpotential generated at gas-evolving electrodes. Electrochim Acta 2005;50:3726–36.
[56] Dukovic J, Tobias CW. The influence of attached bubbles on potential drop and current distribution at gas-evolving electrodes. J Electrochem Soc 1987;134:331–43.
[57] Vogt H. The concentration overpotential of gas evolving electrodes as a multiple problem of mass transfer. J Electrochem Soc 1990;137:1179–84.
[58] Matsushima H, Iida T, Fukunaka Y. Observation of bubble layer formed on hydrogen and oxygen gas-evolving electrode in a magnetic field. J Solid State Electrochem 2012;16:617–23.
[59] Mandin P, Aissa AA, Roustan H, Hamburger J, Picard G. Two-phase electrolysis process: from the bubble to the electrochemical cell properties. Chem Eng Process: Process Intensification 2008;47:1926–32.
[60] Ling WYL, Lu G, Ng TW. Increased stability and size of a bubble on a superhydrophobic surface. Langmuir 2011;27:3233–7.
[61] Liu M, Wang S, Wei Z, Song Y, Jiang L. Bioinspired design of a superoleophobic and low adhesive water/solid interface. Adv Mater 2009;21:665–9.
[62] Yao X, Song Y, Jiang L. Applications of bio-inspired special wettable surfaces. Adv Mater 2011;23:719–34.
[63] Wen L, Tian Y, Jiang L. Bioinspired super-wettability from fundamental research to practical applications. Angew Chem Int Ed 2015;54:3387–99.
[64] Barati Darband G, Aliofkhazraei M, Khorsand S, Sokhanvar S, Kaboli A. Science and engineering of superhydrophobic surfaces: review of corrosion resistance, chemical and mechanical stability. Arab. J. Chem. 2018. https://doi.org/10.1016/j.arabjc.2018.01.013.
[65] Ma M, Hill RM. Superhydrophobic surfaces. Curr Opin Colloid Interface Sci 2006;11:193–202.
[66] Zhang X, Shi F, Niu J, Jiang Y, Wang Z. Superhydrophobic surfaces: from structural control to functional application. J Mater Chem 2008;18:621–33.
[67] Dorrer C, Rühe Jr.. Superaerophobicity: repellence of air bubbles from submerged, surface-engineered silicon substrates. Langmuir 2012;28:14968–73.
[68] de Maleprade H, Clanet C, Quéré D. Spreading of bubbles after contacting the Lower side of an aerophilic slide immersed in water. Phys Rev Lett 2016;117:094501.
[69] Faber MS, Dziedzic R, Lukowski MA, Kaiser NS, Ding Q, Jin S. High-performance electrocatalysis using metallic cobalt pyrite (CoS2) micro-and nanostructures. J Am Chem Soc 2014;136:10053–61.
[70] Xu W, Lu Z, Wan P, Kuang Y, Sun X. High-performance water electrolysis system with double nanostructured superaerophobic electrodes. Small 2016;12:2492–8.
[71] Wang J, Zheng Y, Nie F-Q, Zhai J, Jiang L. Air bubble bursting effect of lotus leaf. Langmuir 2009;25:14129–34.
[72] Lu Z, Li Y, Lei X, Liu J, Sun X. Nanoarray based “superaerophobic” surfaces for gas evolution reaction electrodes. Materials Horizons 2015;2:294–8.
[73] Zhang P, Wang S, Wang S, Jiang L. Superwetting surfaces under different media: effects of surface topography on wettability. Small 2015;11:1939–46.
[74] Huang Y, Liu M, Wang J, Zhou J, Wang L, Song Y, et al. Controllable underwater oil-adhesion-interface films assembled from nonspherical particles. Adv Funct Mater 2011;21:4436–41.
[75] Chen X, Wu Y, Su B, Wang J, Song Y, Jiang L. Terminating marine methane bubbles by superhydrophobic sponges. Adv Mater 2012;24:5884–9.
[76] Hao J, Yang W, Huang Z, Zhang C. Superhydrophilic and superaerophobic copper phosphide microsheets for efficient electrocatalytic hydrogen and oxygen evolution. Adv Mater Interfaces 2016;3:1600236.
[77] Zhang Q, Li P, Zhou D, Chang Z, Kuang Y, Sun X. Superaerophobic ultrathin Ni–Mo alloy nanosheet array from in situ topotactic reduction for hydrogen evolution reaction. Small 2017;13.
[78] Li Y, Zhang H, Xu T, Lu Z, Wu X, Wan P, et al. Under-water superaerophobic pine-shaped Pt nanoarray electrode for ultrahigh-performance hydrogen evolution. Adv Funct Mater 2015;25:1737–44.
[79] Ang H, Tan HT, Luo ZM, Zhang Y, Guo YY, Guo G, et al. Hydrophilic nitrogen and sulfur Co-doped molybdenum carbide nanosheets for electrochemical hydrogen evolution. Small 2015;11:6278–84.
[80] Xu Y-T, Xiao X, Ye Z-M, Zhao S, Shen R, He C-T, et al. Cage-confinement pyrolysis route to ultrasmall tungsten carbide nanoparticles for efficient electrocatalytic hydrogen evolution. J Am Chem Soc 2017;139:5285–8.
[81] Liu Q, Tian J, Cui W, Jiang P, Cheng N, Asiri AM, et al. Carbon nanotubes decorated with CoP nanocrystals: a highly active non-noble-metal nanohybrid electrocatalyst for hydrogen evolution. Angew Chem Int Ed 2014;53:6710–4.
[82] Feng G, Kuang Y, Li Y, Sun X. Three-dimensional porous superaerophobic nickel nanoflower electrodes for high-performance hydrazine oxidation. Nano Research 2015;8:3365–71.
[83] Akbar K, Kim JH, Lee Z, Kim M, Yi Y, Chun S-H. Superaerophobic graphene nanohills for direct hydrazine fuel cells. NPG Asia Mater 2017;9:e378.
[84] Jiang M, Wang H, Li Y, Zhang H, Zhang G, Lu Z, et al. Superaerophobic RuO2-based nanostructured electrode for high-performance chlorine evolution reaction. Small 2017;13.
[85] Kuang Y, Feng G, Li P, Bi Y, Li Y, Sun X. Single-crystalline ultrathin nickel nanosheets array from in situ topotactic reduction for active and stable electrocatalysis. Angew Chem Int Ed 2016;55:693–7.
[86] Li Y, Wang H, Xie L, Liang Y, Hong G, Dai H. MoS2 nanoparticles grown on graphene: an advanced catalyst for the hydrogen evolution reaction. J Am Chem Soc 2011;133:7296–9.
[87] Hinnemann B, Moses PG, Bonde J, Jørgensen KP, Nielsen JH, Horch S, et al. Biomimetic hydrogen evolution: MoS2 nanoparticles as catalyst for hydrogen evolution. J Am Chem Soc 2005;127:5308–9.
[88] Voiry D, Salehi M, Silva R, Fujita T, Chen M, Asefa T, et al. Conducting MoS2 nanosheets as catalysts for hydrogen evolution reaction. Nano Lett 2013;13:6222–7.
[89] Lu Z, Zhu W, Yu X, Zhang H, Li Y, Sun X, et al. Ultrahigh hydrogen evolution performance of under-water “superaerophobic” MoS2 nanostructured electrodes. Adv Mater 2014;26:2683–7.
[90] Zhang Q, Li P, Zhou D, Chang Z, Kuang Y, Sun X. Superaerophobic ultrathin Ni–Mo alloy nanosheet array from in situ topotactic reduction for hydrogen evolution reaction. Small 2017;13:1701648.
[91] Li Y, Zhang H, Jiang M, Zhang Q, He P, Sun X. 3D self-supported Fe-doped Ni2P nanosheet arrays as bifunctional catalysts for overall water splitting. Adv Funct Mater 2017;27:1702513.
[92] Li Y, Zhang H, Jiang M, Kuang Y, Sun X, Duan X. Ternary NiCoP nanosheet arrays: an excellent bifunctional catalyst for alkaline overall water splitting. Nano Research 2016;9:2251–9.
[93] Xi W, Yan G, Tan H, Xiao L, Cheng S, Khan SU, et al. Superaerophobic P-doped Ni (OH) 2/NiMoO 4 hierarchical nanosheet arrays grown on Ni foam for electrocatalytic overall water splitting. Dalton Trans 2018;47:8787–93.
[94] Tian Y, Yu J, Zhang H, Wang C, Zhang M, Lin Z, et al. 3D porous Ni-Co-P nanosheets on carbon fiber cloth for efficient hydrogen evolution reaction. Electrochim Acta 2019;300:217–24.
[95] Sun H, Xu X, Yan Z, Chen X, Jiao L, Cheng F, et al. Superhydrophilic amorphous Co–B–P nanosheet electrocatalysts with Pt-like activity and durability for the hydrogen evolution reaction. J Mater Chem 2018;6:22062–9.

[96] Barati Darband G, Aliofkhazraei M, Sabour Rouhaghdam A. Three-dimensional porous Ni-CNT composite nanocones as high performance electrocatalysts for hydrogen evolution reaction. J Electroanal Chem 2018;829:194–207.
[97] Lotfi N, Farahani TS, Yaghoubinezhad Y, Darband GB. Simulation and characterization of hydrogen evolution reaction on porous NiCu electrode using surface response methodology. Int J Hydrogen Energy 2019;44:13296–309.
[98] Barati Darband G, Aliofkhazraei M, Rouhaghdam AS. Facile electrodeposition of ternary Ni-Fe-Co alloy nanostructure as a binder free, cost-effective and durable electrocatalyst for high-performance overall water splitting. J Colloid Interface Sci 2019;547:407–20.
[99] Lu X, Zhao C. Electrodeposition of hierarchically structured three-dimensional nickel–iron electrodes for efficient oxygen evolution at high current densities. Nat Commun 2015;6:6616.
[100] Liu T, Xie L, Yang J, Kong R, Du G, Asiri AM, et al. Self-standing CoP nanosheets array: a three-dimensional bifunctional catalyst electrode for overall water splitting in both neutral and alkaline media. ChemElectroChem 2017;4:1840–5.
[101] Wang J, Zhong H-x, Wang Z-l, Meng F-l, Zhang X-b. Integrated three-dimensional carbon paper/carbon tubes/cobalt-sulfide sheets as an efficient electrode for overall water splitting. ACS Nano 2016;10:2342–8.
[102] Suen N-T, Hung S-F, Quan Q, Zhang N, Xu Y-J, Chen HM. Electrocatalysis for the oxygen evolution reaction: recent development and future perspectives. Chem Soc Rev 2017;46:337–65.
[103] Li CW, Ciston J, Kanan MW. Electroreduction of carbon monoxide to liquid fuel on oxide-derived nanocrystalline copper. Nature 2014;508:504.
[104] Wang L, Huang X, Jiang S, Li M, Zhang K, Yan Y, et al. Increasing gas bubble escape rate for water splitting with nonwoven stainless steel fabrics. ACS Appl Mater Interfaces 2017;9:40281–9.
[105] He J, Hu B, Zhao Y. Superaerophobic electrode with metal@ metal-oxide powder catalyst for oxygen evolution reaction. Adv Funct Mater 2016;26:5998–6004.
[106] Han N, Yang KR, Lu Z, Li Y, Xu W, Gao T, et al. Nitrogen-doped tungsten carbide nanoarray as an efficient bifunctional electrocatalyst for water splitting in acid. Nat Commun 2018;9:924.
[107] Li H, Chen S, Zhang Y, Zhang Q, Jia X, Zhang Q, et al. Systematic design of superaerophobic nanotube-array electrode comprised of transition-metal sulfides for overall water splitting. Nat Commun 2018;9:2452.
[108] Akbar K, Hussain S, Truong L, Roy SB, Jeon JH, Jerng S-K, et al. Induced superaerophobicity onto a non-superaerophobic catalytic surface for enhanced hydrogen evolution reaction. ACS Appl Mater Interfaces 2017;9:43674–80.
[109] Yu X, Yu Z-Y, Zhang X-L, Zheng Y-R, Duan Y, Gao Q, et al. “Superaerophobic” nickel phosphide nanoarray catalyst for efficient hydrogen evolution at ultrahigh current densities. J Am Chem Soc 2019;141:7537–43.
[110] Balram A, Zhang H, Santhanagopalan S. Enhanced oxygen evolution reaction electrocatalysis via electrodeposited amorphous α-phase nickel-cobalt hydroxide nanodendrite forests. ACS Appl Mater Interfaces 2017;9:28355–65.
[111] Sun J, Chen Y, Ren Z, Fu H, Xiao Y, Wang J, et al. Self-Supported NiS nanoparticle-coupled Ni2P nanoflake array architecture: an advanced catalyst for electrochemical hydrogen evolution. ChemElectroChem 2017;4:1341–8.
[112] Koza JA, Mühlenhoff S, Żabiński P, Nikrityuk PA, Eckert K, Uhlemann M, et al. Hydrogen evolution under the influence of a magnetic field. Electrochim Acta 2011;56:2665–75.
[113] Matsushima H, Iida T, Fukunaka Y. Gas bubble evolution on transparent electrode during water electrolysis in a magnetic field. Electrochim Acta 2013;100:261–4.
[114] Lin M-Y, Hourng L-W, Kuo C-W. The effect of magnetic force on hydrogen production efficiency in water electrolysis. Int J Hydrogen Energy 2012;37:1311–20.
[115] Monzon LM, Coey JMD. Magnetic fields in electrochemistry: the Lorentz force. A mini-review. Electrochem Commun 2014;42:38–41.
[116] De Andrade V, Pereira J. Gravitational Lorentz force and the description of the gravitational interaction. Phys Rev D 1997;56:4689.
[117] Vogt H, Balzer R. The bubble coverage of gas-evolving electrodes in stagnant electrolytes. Electrochim Acta 2005;50:2073–9.
[118] Aogaki R, Fueki K, Mukaibo T. Application of magnetohydrodynamic effect to the analysis of electrochemical reactions. 2. diffusion process in mhd forced flow of electrolyte solution. Denki kagaku 1975;43:509–14.
[119] Diao Z, Dunne P, Zangari G, Coey J. Electrochemical noise analysis of the effects of a magnetic field on cathodic hydrogen evolution. Electrochem Commun 2009;11:740–3.
[120] Elias L, Hegde AC. Effect of magnetic field on HER of water electrolysis on Ni–W alloy. Electrocatalysis 2017;8:375–82.
[121] Wang C-C, Chen C-Y. Water electrolysis in the presence of an ultrasonic field. Electrochim Acta 2009;54:3877–83.
[122] Wang M, Wang Z, Guo Z. Understanding of the intensified effect of super gravity on hydrogen evolution reaction. Int J Hydrogen Energy 2009;34:5311–7.
[123] Guo Z, Gong Y, Lu W. Electrochemical studies of nickel deposition from aqueous solution in super-gravity field. Sci China Ser E Technol Sci 2007;50:39–50.
[124] Cheng H, Scott K. An empirical model approach to gas evolution reactions in a centrifugal field. J Electroanal Chem 2003;544:75–85.
[125] Wang M-y, XING H-Q, Wang Z, GUO Z-C. Investigation of chlor-alkali electrolysis intensified by super gravity. Acta Physico-Chim Sin 2008;24:520–6.
[126] Mat MD, Aldas K. Application of a two-phase flow model for natural convection in an electrochemical cell. Int J Hydrogen Energy 2005;30:411–20.
[127] Cheng H, Scott K, Ramshaw C. Intensification of water electrolysis in a centrifugal field. J Electrochem Soc 2002;149:D172–7.
[128] Wang M, Wang Z, Guo Z. Water electrolysis enhanced by super gravity field for hydrogen production. Int J Hydrogen Energy 2010;35:3198–205. ss.